Human Powered Aircraft for Sport

AOE 4066 – Virginia Polytechnic Institute and State University
Final Report: Spring Semester – May 11, 2009

Dr. William Mason	*Faculty Advisor*
Mark Hollinshead	*Project Manager*
James Dorman	*Wings*
Brett Layton	*Propulsion/Drivetrain*
Kristen Moore	*Structures*
Fred McMahon	*Cockpit*
Michael Smith	*Cockpit/Drivetrain/Dyno*
Masato Nakagawa	*Tail*
Jennifer Prall	*Weights*
Jonathan Murrow	*Newsletters/Wings*
Valeriy Vislobokov	*Drivetrain/IT*
Scott Hutchinson	*Cockpit*
Rosa Avalos	*Cockpit/Materials*

Table of Contents

1. Executive Summary

The Virginia Tech Human Powered Aircraft Group is presently in the fourth year of designing and advancing the development of an aircraft aimed at winning one of the current Kremer Prizes. After three years of preliminary and detail design, the project is in the building, testing, and redesigning iteration phase.

This report details the current design of the entire aircraft and is a compilation of work from the 2008-2009 team in the Spring 2009 semester. This document begins with a brief orientation to the project, including an introduction to the Kremer Prize.

The body of the report is split into three sections. Section 3 is the prototype design that has taken place throughout this year, section 4 is the construction details and section 5 is the testing of various components. The report concludes with a brief status report, an overview of the administrative details, and finally a brief summary of the report as well as references.

2. Introduction

2.1 HPA Background

The catalyst for most human-powered aircraft (HPA) activity for the past 40 years or so has been the Kremer Prizes offered by the Royal Aeronautical Society (RAS). The competitions have dictated the design criteria for most HPA's since the advent of the prize in 1959. The first successful HPA was Paul MacCready's Gossamer Condor, which won the first Kremer Prize in 1977; 18 years after the prize had been introduced. Many of the early HPA attempts were based on emulating sailplanes. MacCready changed the direction and expanded on the concepts used in hang-gliders to create the first successful HPA.

MacCready also won the next Kremer Prize only two years later in 1979 with the Gossamer Albatross, which crossed the English Channel. Five years later the RAS offered a new prize based on aircraft speed, the rules for which allowed ten minutes of energy storage by the pilot prior to the flight. There were two main competitors for the speed prize, MacCready and a group of students from MIT. The MIT group successfully flew their entry, Monarch, to win the prize.

There have been several successful HPA's not associated with the Kremer Prize, including MIT's Chrysalis and Daedalus. The designs of many of the successful HPA have several similar characteristics. The first and very important similarity is the pilot seating position. In all but the Condor, the pilot is seated in a recumbent position. This position proves to be much better for power production than the upright position. Another important similarity is the aft tail on all but the two Gossamer aircraft. With the exception of Chrysalis, which was a biplane, all other HPA's have high and generally straight wings. All HPA's except Daedalus have had ailerons. They were cut from Daedalus because its mission required almost no turning, resulting in a small weight reduction.

There are currently three Kremer prizes available, each for a monetary prize. The first is the Kremer International Marathon Competition, which challenges the competitor to fly a 26 mile marathon course in less than an hour. The second competition is the Kremer Human-Powered Aircraft for Sport Competition stressing maneuverability. The competition goal is to design a Human-Powered Aircraft that could be used in an Arial Sporting event around an equilateral triangular course of 500m on each side. The third competition is limited to universities in the UK. [1]

2.2 The Kremer Prize for Sport

2.2.1 Human-powered Aircraft for Sport Competition

The overall goal of this project is the completion of the Human-Powered Aircraft for Sport challenge hosted by the Royal Aeronautical Society. The purpose of this challenge is to bring forth the creation of a sport from this class of airplane. A reward of £100,000 will be presented to the first entrant that is capable of demonstrating flight that meets the requirements of the competition.

The aircraft requirements for this prize are:

- The aircraft has to operate safely at low altitudes, close to the ground, and be well disposed to kit production.
- Flown by one individual that uses muscular power for propulsion.
- No batteries or electric cells can be used to store energy for propulsion.
- No lighter than air gasses can be used to generate lift.
- The entire aircraft must be stored in a trailer with a maximum length of 8 meters.
- No part of the aircraft can be discarded on or after takeoff.

2.2.2 Competition Course

The Human-Powered Aircraft has a specific course that must be adhered to in order to successfully complete the competition [2]. This course is displayed in the Figure 2.2.2. The

course may be anywhere in the UK, either over land or water, such that it meets the following criteria:

- The course is an equilateral triangle 500m on each side.
- The course shall be flown both clockwise and counter clockwise.
- The plane shall fly at least 5m off the ground.
- The mean wind speed during flight will not be less than 5 m/s.
- The wind speed will not drop below 5 m/s for more than 20s during flight or the flight will be void.

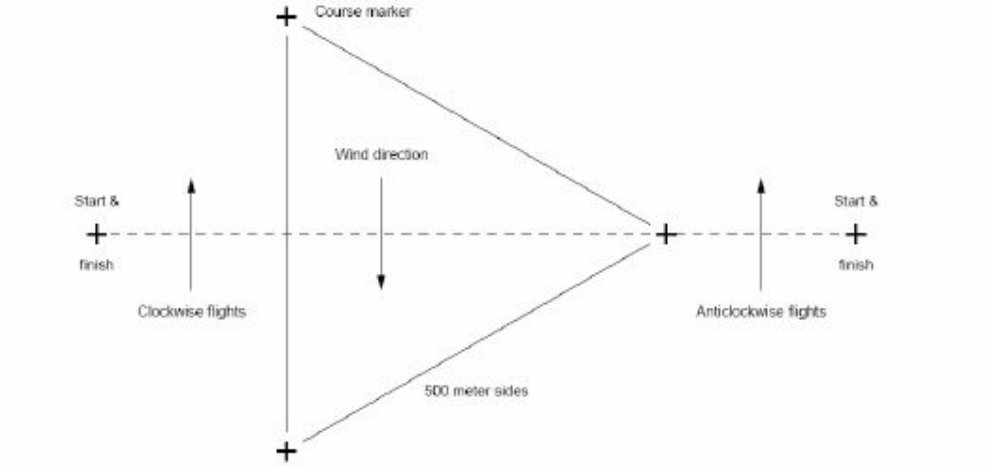

Figure 2.2.2: Kremer Prize for Sport Competition Course Diagram

2.3 Previous Project Development

Because this project is currently in its fourth year of development, this team must study and understand thoroughly what previous teams have accomplished. The current team was required to pick up where our predecessors left off, while still keeping in mind that previous designs may need to be tweaked or perhaps changed all together. The following sections will give a brief description of the previous project development.

2.3.1 2005-2006 HPA Team

The fall of 2005 was the year that the Human Powered Aircraft Group was formed and began conceptual design on an aircraft to eventually compete for the Kremer prize. To properly begin conceptual design, constraints were defined based on the rules for the

competition and a mission analysis, which determined how the aircraft and pilot would need to perform during flight. Next, the team considered several conceptual design sketches and ranked them using a design matrix. Two of the top designs were considered for further analysis; a monoplane and a box-wing configuration.

Aerodynamically, the team found that the box-wing configuration was the better of the two options. Using the design constraints, the wing area was selected. They then concentrated on finding airfoils that would perform the best for the wing and tail surfaces with minimal drag.

Structurally, the team considered each of the two concept configurations by building and testing simple models. After finding the box-wing configuration was superior, finite element analysis was performed to optimize the design. Basic structural design such as number of struts and gap width between wings were also analyzed to minimize drag.

The first year's team began some preliminary design regarding the propulsion system. After researching previous HPA's a basic drive train was designed that resembled that of a bicycle. Pilot positioning was also researched and an optimal position was chosen. The team also designed a propeller for use with a variable pitch mechanism in order to provide the optimal propeller pitch at different flight conditions.

The latter half of the year was consumed with constructing and testing a quarter scale model of the aircraft. The model was built primarily to test and validate the dynamic stability and control of the aircraft. The wing structures were constructed with some built-in deflection to make the wing perform like the full-scale aircraft. The model was scaled so that it would behave dynamically similar to the full-scale model [4].

Figure 2.3.1 is a simple computer model that shows how the first year's team envisioned the HPA.

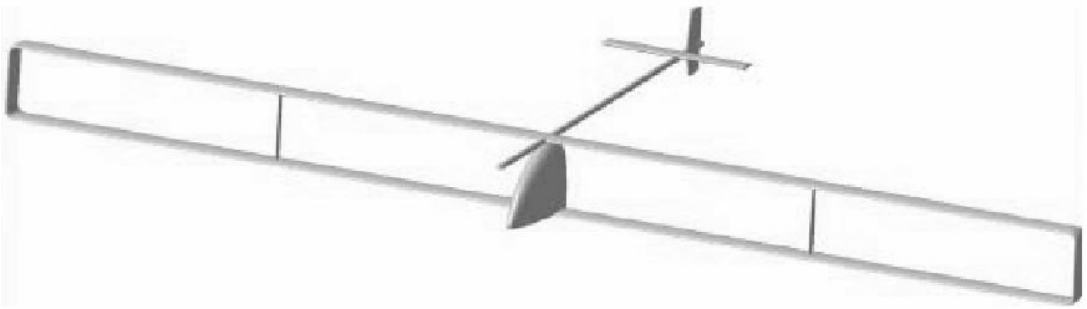

Figure 2.3.1: Computer model of 1st teams design [4]

2.3.2 2006-2007 HPA Team

The second year HPA team picked up where the first year's team left off, and focused the entire first semester in further developing the quarter scale model. Aerodynamic problems existed with the model in the first year, as documented by the flight test videos and reports. Because of this, the team performed more aerodynamic and stability and control analyses to help provide them with a blueprint for model modifications. Other structural analysis was also performed using computer simulations to help modify the existing design.

After performing this analysis, there were four major concerns the team had regarding the model. These were replacing the original carbon fiber fuselage, addition of guy wires, construction of a new elevator, and the addition of landing gear. Upon completion of these design and construction issues, the second year team began testing the quarter scale model. The flight tests were much improved from the previous year and resulted in the model performing several 360^{o} turns.

Although much of the conceptual design and some detailed design was completed by the previous team, the 2006-2007 team focused their detail design on optimizing the structural aspects of the aircraft, and performing detailed aerodynamic design. In the second semester, along with continued detail design, the second year team began construction of a full-scale prototype with the hope of beginning flight-testing in the spring of 2007. With full-

scale construction in mind, the team also began to acquire funds and workspace during the second semester.

In terms of the design, the team reached their goals of finalizing the spar, strut and airfoil design, while continuing to improve the overall detailed design of the aircraft. The team did not, however, complete construction of the full-scale prototype. Multiple wing sections have been built and tested, but the construction processes have not yet been perfected [5].

2.3.3 2007-2008 HPA Team

The 2007-2008 team began testing both the wing's structural integrity as well as the propeller efficiency. The structural testing showed discrepancies between the ANSYS analysis made by the 2006-2007 team and the testing conducted by the 2007-2008 team. The team focused a lot of effort at resolving these issues.

Further more, this team built both the propeller as well as a testing device to investigate the efficiency of the propeller. Unfortunately, there were thrust reading issues with the dynamometer system developed which are still being worked out by the 2008-2009 team.

2.4 Mission Objectives

The 2008-2009 team has continued with the efforts of re-testing the wings, testing of the propeller, construction of the horizontal and vertical tails, updated CAD models, ANSYS analysis on the cockpit, redesign of the cockpit, and developing a new propeller/drive train test vehicle. There have been many obstacles this semester in working towards the completion of these goals. A major stumbling block for this year's team has been the lack of detailed design by previous years which has hindered the construction process.

3. Prototype Design

3.1 Cockpit

3.1.1 Current Design

The current cockpit design calls for the cockpit framework to be made to the dimensions shown in Figure 3.1.1. The framework will be made out of aluminum or carbon fiber tubes, depending on how the results of the structural analysis, with an outer diameter of 2 inches, and a thickness of 0.032 inches.

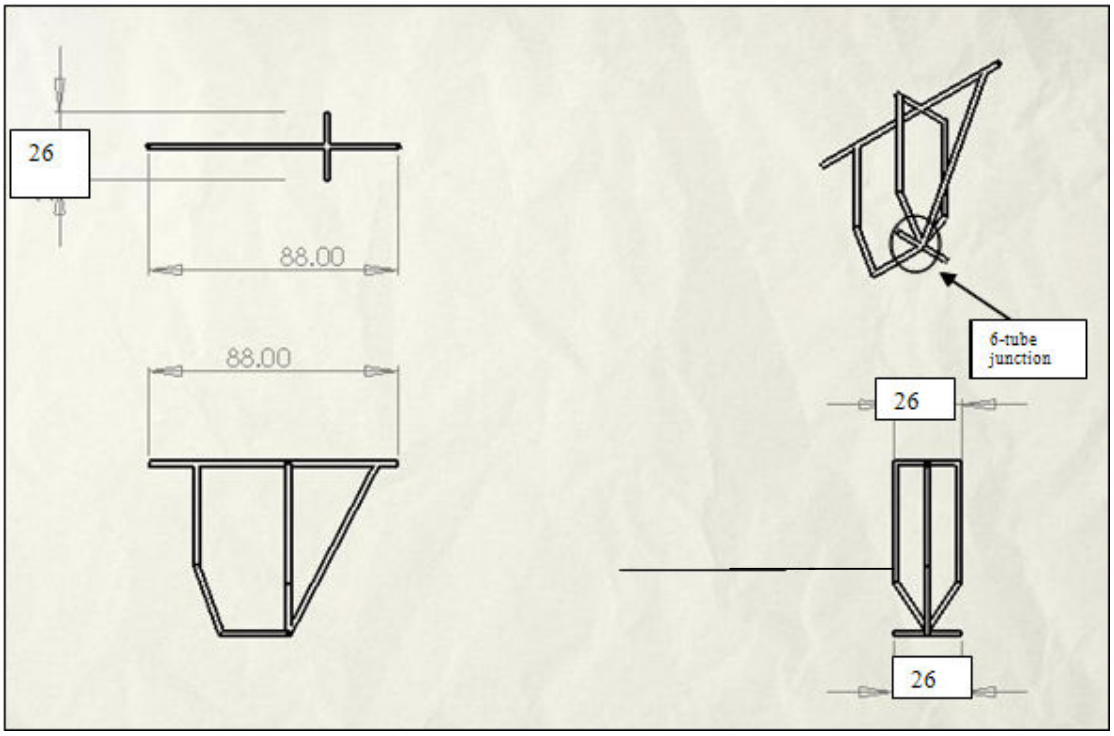

Figure 3.1.1-1: Three View sketch of Cockpit, all dimensions are in inches

It is possible the tube outer diameter and thickness may change if the structural analysis suggests such a change will not adversely affect the structural integrity of the airplane. A major problem with this design is the 6-tube junction, as shown in Figure 3.1.1-1. Since there are six tubes coming together to one point, this will pose a serious problem during the construction process.

3.1.2 Dimensions Confirmation

The first task for this year's team was to confirm the dimensions of the cockpit and adjust any of the dimensions, if necessary. Any of the dimensions found on the cockpit design that were not perfect decimals, i.e. could easily be converted to the nearest 1/16th of an inch, are listed in Table 3.1.2-1. Those dimensions are then converted to the nearest 1/16th of an inch, in order to determine if any changes to the dimensions are needed. In order to change the dimensions, there needs to be a significant difference in the actual dimension and the nearest 16th of an inch dimension.

Table 3.1.2-1: Analysis of changing tube lengths

Type of Tube	Actual Tube Length	Tube Length to the nearest 1/16"	% Difference
Diagonal	25.5403	25.5625	-0.09%
Horizontal	25.6237	25.625	-0.01%
Diagonal	26.8328	26.8125	0.08%
Horizontal	34.359	34.375	-0.05%
Horizontal	34.641	34.625	0.05%
Diagonal	69.282	69.3125	-0.04%

As can be seen from Table 3.1.2-1, the differences in the tube lengths really are not significant, and can be changed to more realistic number values when a construction plan is made. Because the differences in the lengths are not significant it was decided to leave the dimensions the way they are until the construction plan is made.

3.1.3 Structural Analysis

The next step of confirming the current cockpit design was to do structural analysis on the cockpit. Previous year's teams did structural analysis on the cockpit using the program CosmoWorks; however this year's team decided to use ANSYS 11.0 for the structural analysis. A couple of weeks were used learning how to use ANSYS 11.0 [1] since there were no current members on the team that knew how to use this structural analysis program. Once the program was learned, we began to run ANSYS for a basic loading set up as determined by previous year's teams [6]. This loading setup, as can be seen from Figure

3.1.3-1, is not complete as it is still missing the weight and reactions from the landing gear, it is missing the lifting forces on the top and bottom bars that connect the cockpit to the wing, and it does not include the correct seat and pedal positions, so the forces on those two locations are not completely accurate. However, there was enough information to generate a basic structural analysis test and allow for this year's team to produce a program [Program 1] that will allow for any changes to be made easily. This program is a script text file that will input all the key points of the cockpit design and then connect those key points in a way that creates the cockpit shape, as can be seen in Figures 3.1.3-1, 3.1.3-2 and 3.1.3-3. The program will then place the forces and moments on the desired key point, constrain the cockpit from movement, and then run the structural analysis. The results of the structural analysis can be seen in Figures 3.1.3-2 and 3.1.3-3.

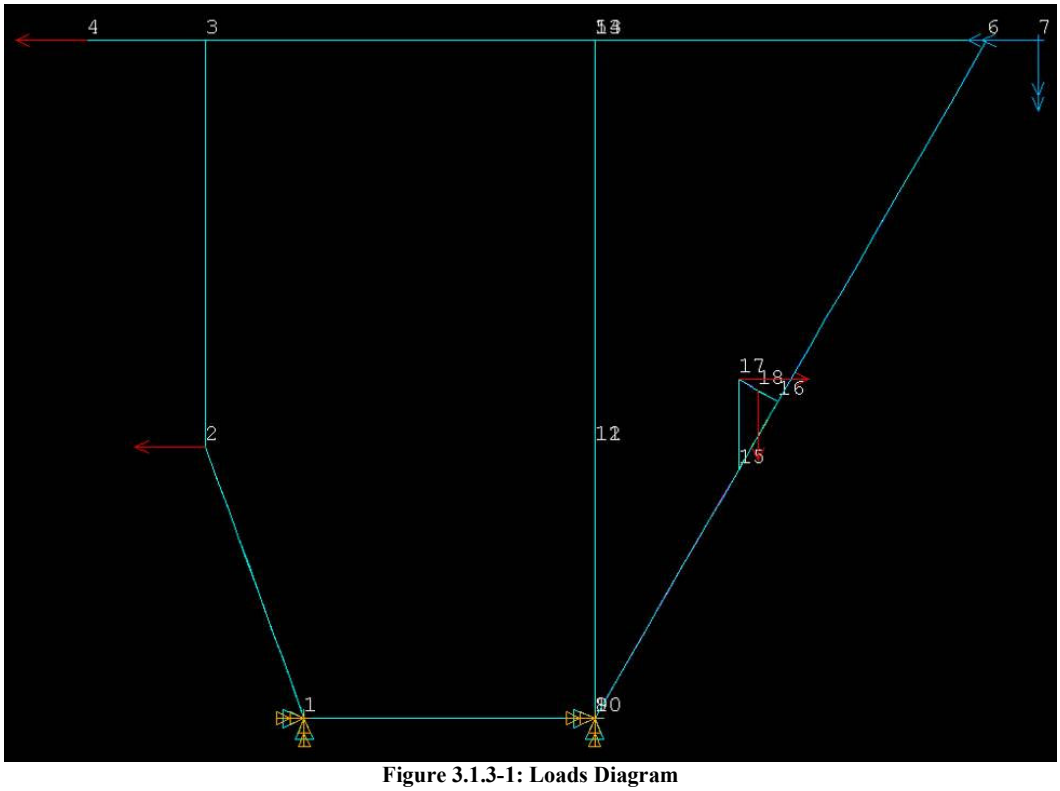

Figure 3.1.3-1: Loads Diagram

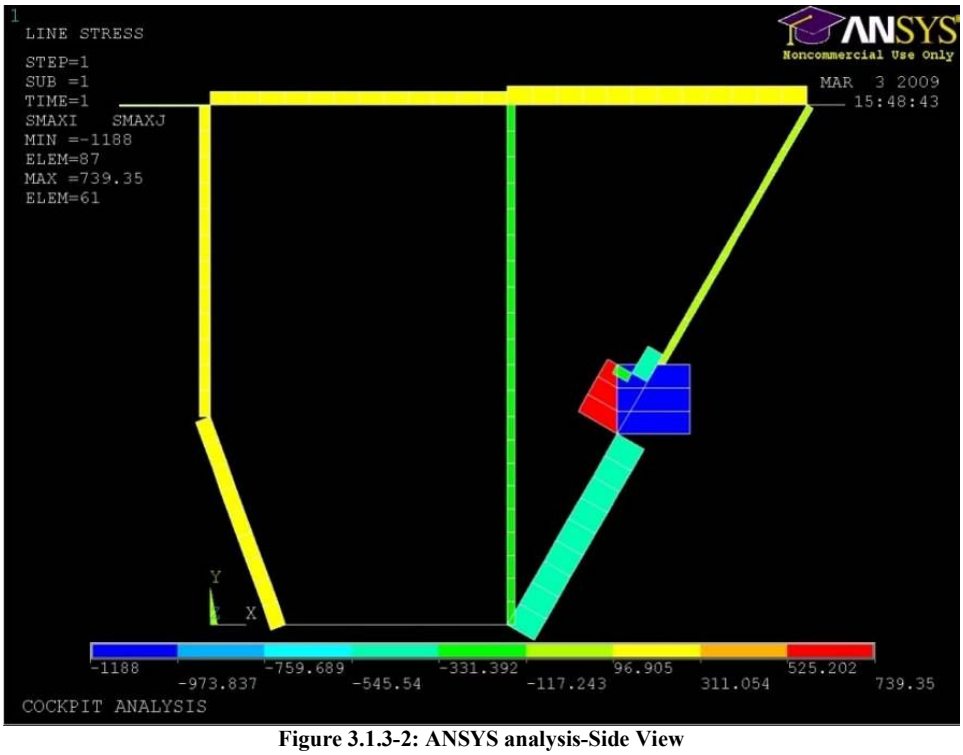

Figure 3.1.3-2: ANSYS analysis-Side View

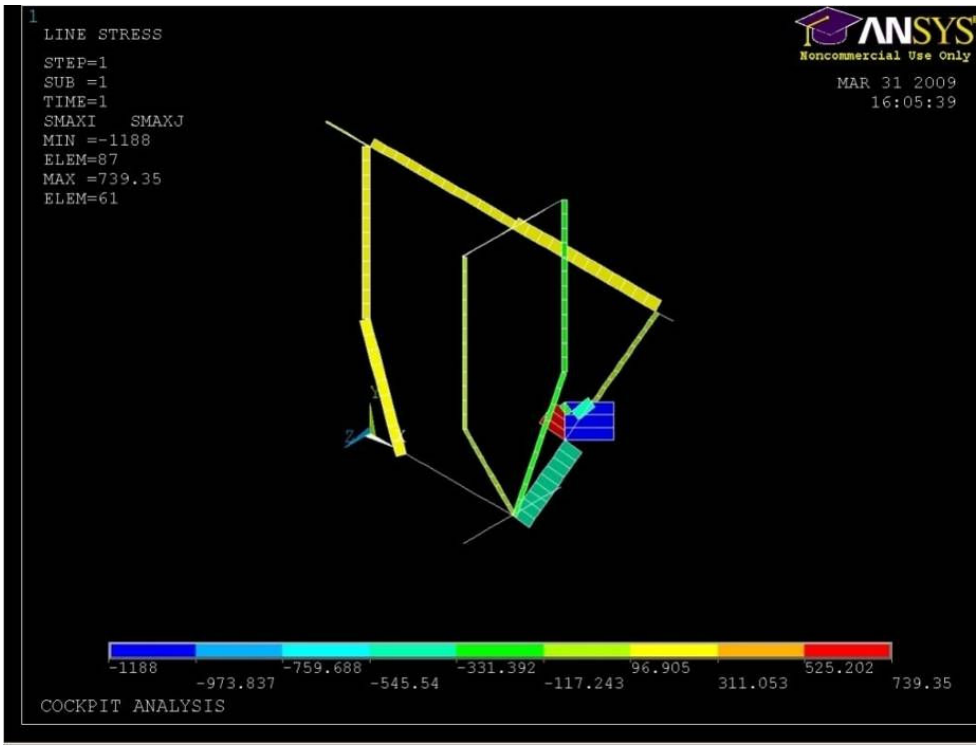

Figure 3.1.3-3: ANSYS analysis-Isometric View

As can be seen in Figure 3.1.3-2 and 3.1.3-3, most of the stresses on the cockpit framework are occurring at the location of the seat. This makes sense because there are large

(140 lbs and 85 lbs) being applied on the seat. Since this is not a full structural analysis yet, as stated above, there are not many conclusions that can be drawn from this; however one conclusion that can be drawn from this analysis is that careful consideration must be made with how the seat is connected to the rest of the cockpit because of the large tensile and compressive stresses being applied. It will also be important to properly support the large junction of structural tubes, as was shown in Figure 3.1.1-1, because of the number of tubes coming together into one point.

3.1.4 Cockpit Airfoil

The current airfoil design calls for using a Van de Vooren airfoil with a 17 percent thickness with 44^{o} trailing edge [6]. This airfoil has a chord length of 8.349 feet and is expected to generate a drag of 0.361 lbs. The airfoil's material will be the same material as the wing airfoil, which is Dura-Lar. The airfoil will wrap around the cockpit, and will start at the forward most point of the cockpit and end 2.22 feet behind the cockpit structure.

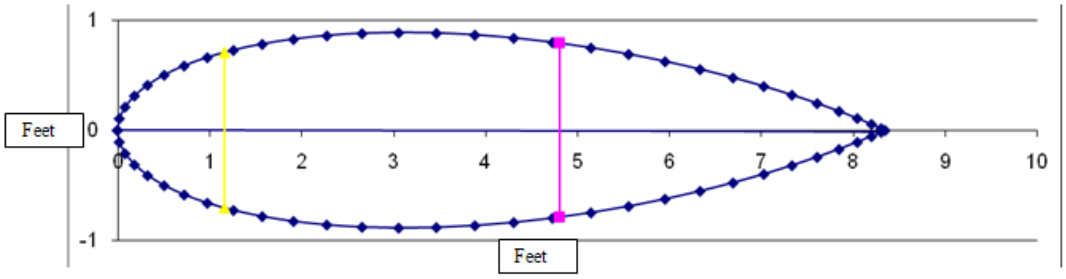

Figure 3.1.5-1: Van de Vooren airfoil with a 17% thickness with 44^{o} trailing edge

The yellow line on Figure 3.1.5-1 represents the width of the airfoil at that point, which is 17 inches. This width is the minimum width necessary to fit a pilot's feet in a cycling motion. The pink line on Figure 3.1.5-1 represents the width of the airfoil at that point, which is 19 inches. This width is the minimum width necessary to fit a pilot's shoulders when seated in the semi-recumbent position.

The problem with the current design is where the pedals will be located in the cockpit. The pedals need to be as far forward as possible because of the forces and moments they will

put on the drive train system, but are restricted by the airfoil and can only come as far forward as 22 inches. This distance is due to the point on the airfoil that has a width of 17 inches will have a length of 14 inches, and the length of the pedal crank is 8 inches. Since the pilot will pedal in a circular motion, the pedals cannot be placed 14 inches from the start of the airfoil, but must be placed 22 inches from the start of the airfoil. Figure 3.1.4-2 shows the problems of the pilot's feet coming into contact with the airfoil that is wrapped around the cockpit.

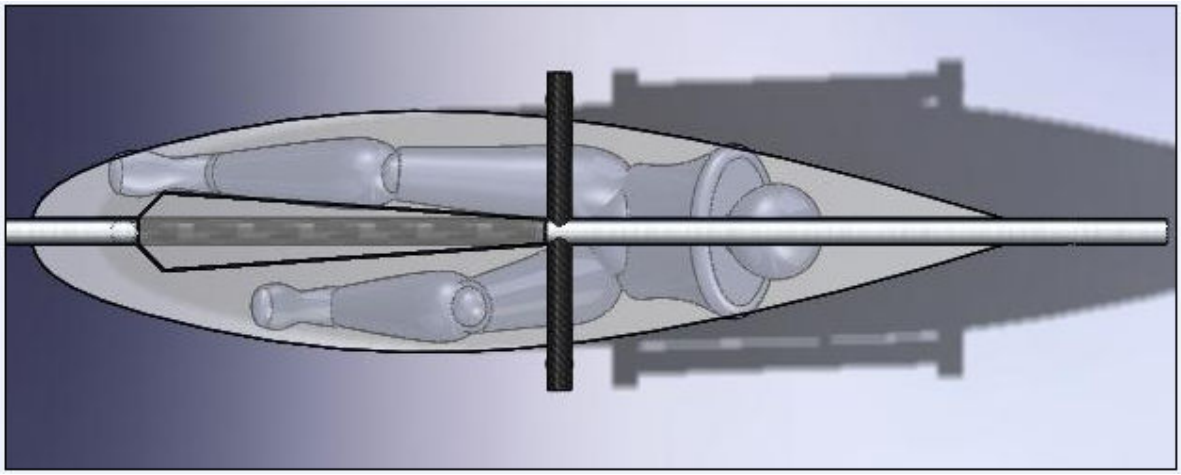

Figure 3.1.4-2: Forward limit of the pilot's feet

One way of working around this restriction is to move the airfoil starting point from the original starting point, the front of the cockpit, to some distance in front of the cockpit. This would allow for the pedals to be moved forward by the same distance inches, which would shorten the horizontal distance for the drive train. How far forward the airfoil can be moved will depend on what length for the propeller shaft this year's and future's years teams are willing to have.

Another problem with the current airfoil design that was discovered is that the widest point on the airfoil with a chord length of 8.349 feet is 21.37 inches, which is 4.63 inches smaller than the widest point for the cockpit. The shortest chord length that will fit the current widest point of the cockpit inside it will be a chord length of 10.5 feet. This causes a

problem for a couple of reasons. The first problem is more material is now needed to cover the cockpit, and there will be roughly four feet of the airfoil off the back of the cockpit. The second problem this causes will be an increase in the expected drag. Currently the drag estimate for an airfoil of chord length 8.349 feet will be 0.361 lbs. By increasing the chord length to 10.5 feet the drag will be increased to 0.454 lbs, which corresponds to a 25.77% increase in the drag on the cockpit. These calculations are shown in Table 3.1.4-1 and the equations used in this table are listed below, where S is the surface area, c is the chord, h is the height of the cockpit, C_D is the drag coefficient, ρ is the density of the fluid, and U_∞ is the velocity of the fluid.

Equation 3.1.4-1

$$S = c \times h$$

Equation 3.1.4-2

$$D = \frac{1}{2} C_D \rho U_\infty^2 S$$

Table 3.1.4-1 Drag information for Cockpit Airfoil

cd	chord	surface area	drag	drag increase
0.0058	8.349	41.7435	0.3608	0.0930
0.0058	10.5	52.5	0.4537	25.77%

While an increase of 0.093 lbs does not seem like a lot, when the airplane's thrust is expected to be at 5.5 lbs, any increase in drag is a bad thing. To fix this problem it is currently being proposed that we make the width of the cockpit 22 inches instead of 26 inches, which should not be a problem. The current ANSYS analysis, as shown in Figures 3.1.3-2 and 3.1.3-3, does not show a large amount of stress in that area, so a decrease in the width should not be a problem.

3.1.5 Seat/Pedal Positioning

The research done by previous teams show that the pilot can generate the most power with his/her legs if their knee bend is somewhere between 90 and 175 degrees. For a typical human of height 70 inches this will correspond to a distance of 34 to 42 inches from the hip

to the pedals. The seat must then be positioned at about a 30° angle to obtain the best visibility and comfort level possible [6].

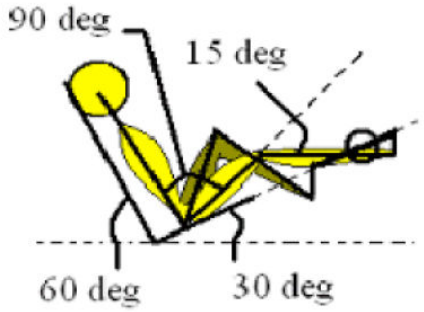

Figure 3.1.5-1: Pilot Positioning [Spring Final Report 07/08-Figure 3.5.1]

The pilot's seat also needs to have the pilot center of gravity as close to the airplane's center of gravity as possible. The airplane's center of gravity is at the 0.4 mean aerodynamic chord and is centered vertically between the two wings [6].

This year's team ran into some problems trying to find a pilot's seat location to correspond to a realistic pedal location that will still keep all the angles and distances at an optimal position; it was determined to be impossible if the cockpit airfoil was not pushed forward. The best position for the seat and the pedals for the current system corresponds to a pedal location of 10 inches from the front of the cockpit and 32 inches from the bottom of the cockpit, a seat location of 7.5 inches from the seven-tube junction and about 13 inches from the bottom of the cockpit, with the airfoil pushed 8 inches forward. This set up will result in a seat angle of exactly 30.8237° and a distance from the hips to the pedals of 37.0993 inches. Since the seat angle is roughly the angle needed, 30°, the seat will be angled at 30° instead of the exact angle measured. The exact positioning of seat and pedals within the cockpit can be seen in Figure 3.1.5-2. This positioning is as optimal as is possible with design, because it does not push the airfoil too far forward, which means the propeller shaft will not be adversely long (it should be roughly 12 inches in length) and because the seat angle and leg distance is within the desired specifications. The program that determined the optimal pilot position was created using Matlab[9]

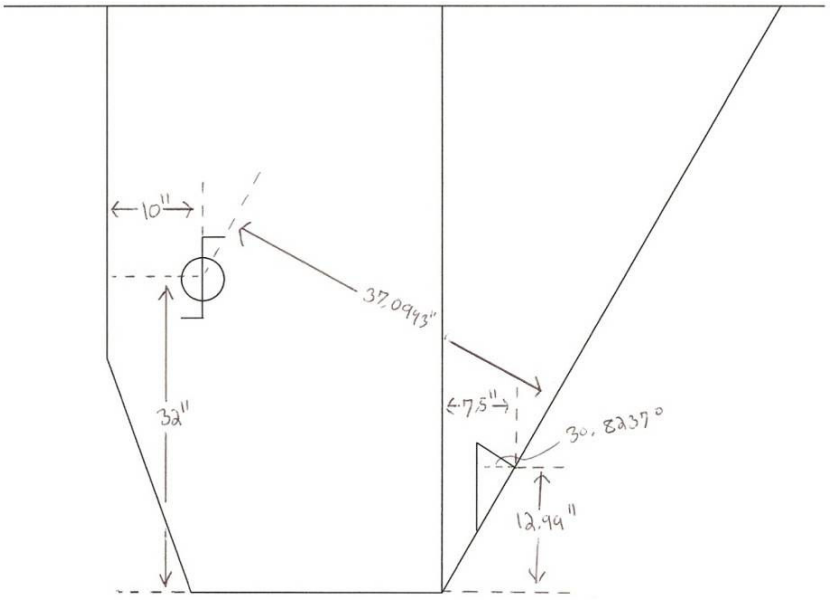

Figure 3.1.5-2: Optimal seat and pedal positioning

While this is optimal for the current design, the seat location is still a little too far away from the airplane's center of gravity point, which could cause some problems during flight. The airplane's center of gravity is desired to be centered with the wings, and the pilot will be sitting 7.5 inches away from the wings. This can be improved with the current set up if the team is willing to have the airfoil pushed out much further than 8 inches, which would cause a much longer propeller shaft. Another way to improve the center of gravity problem is to re-design the cockpit around the concept of having the seat almost right on top of the airplane's center of gravity, and determine where the best location for the pedals is from there.

3.1.6 New Cockpit Design

As the year progressed, it became apparent that the current design of the cockpit needs to be changed to better fit the pilot inside the cockpit and fit the airfoil around the cockpit. The new cockpit design must allow for the pilots center of gravity to be as close to the center of gravity of the airplane as possible. The new design must also allow for the pedals to be in the optimal spot, as close to the front of the cockpit as possible while still

fitting inside the airfoil shape. Finally, the new design must also allow for the cockpit airfoil to not be moved too far forward, which will allow the propeller shaft to be shorter. The new cockpit design is shown in Figure 3.1.6-1. As compared to the original cockpit design, as shown in Figure 3.1.1-1, the new designed lengthened the two top bars and both sides of the wings by 8 inches. Then the front bar is made a straight, vertical bar, instead of the two bars, one vertical and one angled; this was done to make the construction process easier and allow for more room to put the pedals. The width of the cockpit is also changed from 26 inches to 22 inches. This new width will allow the cockpit airfoil's chord length to be 9 feet, which will have a drag of 0.389 lbs. This new design also eliminates the 6-tube junction, and makes it an intersection point of 4 tubes, all on the same plane (no vertical axis), which is much easier to connect all the tubes. With this new design, the pilot's seat can be 0.75 inches from wings, and still allow the pedals to be placed in a position that will allow for all the necessary angles and distances needed. Once the center of gravity of the airplane is confirmed to be at the 0.4 mean aerodynamic chord and is centered vertically between the two wings [6], then the pilot's seat can be placed.

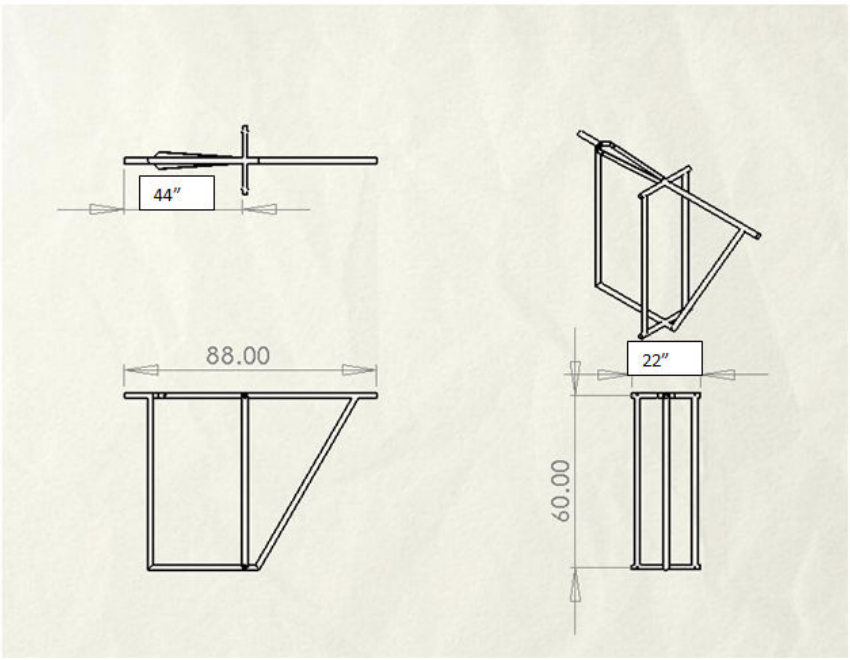

Figure 3.1.6-1: New cockpit design

With a new cockpit design, it became necessary to redo the ANSYS analysis program for this new design, and run a preliminary analysis, using the loading setup as specified in Section 3.1.3. The new loading setup, and new ANSYS analysis pictures are shown in Figure 3.1.6-2, 3.1.6-3 and 3.1.6-4.

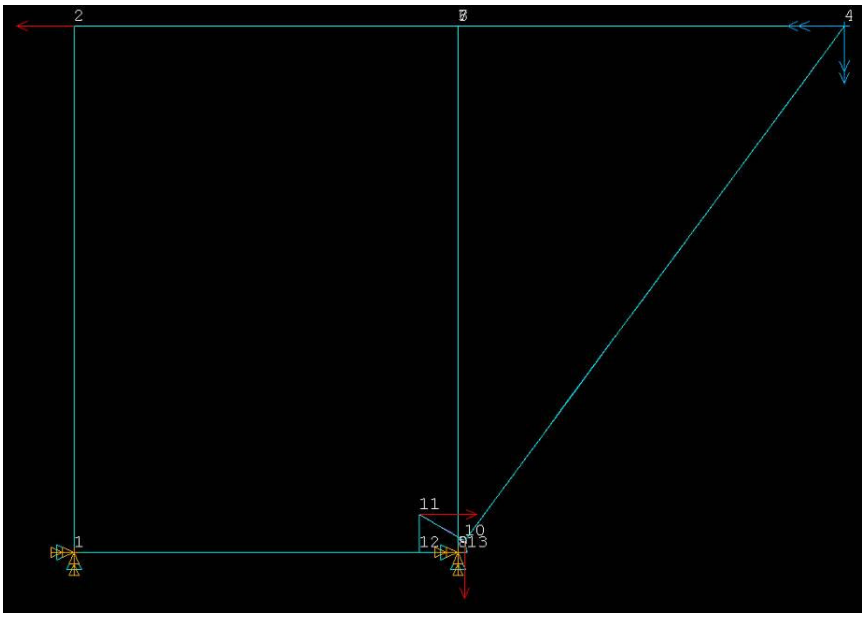

Figure 3.1.6-2: New Loads Setup

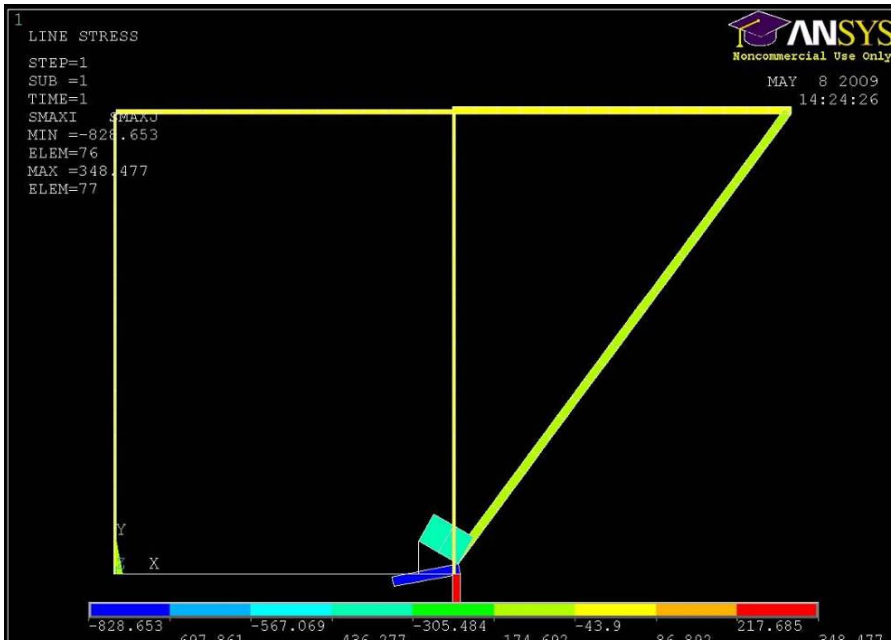

Figure 3.1.6-3: New Front View ANSYS analysis

Figure 3.1.6-4: New Front View ANSYS analysis

3.1.7 Remaining Work to be done

The materials for the cockpit framework need to be determined. It was proposed by previous teams to use Aluminum 6061 tubes with an outer diameter of 2 inches and thickness of 0.032 inches. It is likely that with further ANSYS analysis, the cockpit framework can be made up of Carbon Fiber tubes. Carbon Fiber is superior to Aluminum in terms of its strength and its weight. The increase in strength could allow for the tubes to have an outer diameter that is smaller than the proposed 2 inches and a thickness that is smaller than the proposed 0.032 inches. The carbon fiber will also lower the weight of the cockpit framework by 2.9 lbs. The lower weight will be very helpful because it will allow other crucial areas of the airplane to have more leeway with how much that section weighs.

Work into how all the tubes connect to each other is needed in order to prepare a construction plan. With the current design, the 6-tube junction is a nightmare to try to connect using the limited resources available to the team, and other areas that need tubes connected to each other at an angle present some problems as well. Also, connect Carbon Fiber or Aluminum with the small thicknesses being used presents some problems as well.

The landing gear for the cockpit still needs to be designed. No work was done on this area this year because the landing gear cannot be designed until the seat location is finalized. The reason for this is one set of the landing gear needs to be behind the pilot's center of gravity to keep the airplane upright while it's sitting on the ground. The landing gear also needs to be designed to handle the additional load factors during landing, as well as not increasing the drag profile of the airplane significantly.

Another important area of design to be done is with the cockpit airfoil. Currently the airfoil is designed to be the same chord length throughout the cockpit. If it is possible taper the airfoil, this will help lower the drag of the cockpit and save materials.

One other area of consideration for the cockpit design is how the pilot will control the airplane. It is currently thought that the pilot will use a joystick to control which ailerons move, the rudder movement, and any other areas that need to be controlled by the pilot.

Once all of the above work is done, as well as anything that was not thought of by this year's team, it will be necessary to create a construction plan. This plan is basically a blueprint for how to build the cockpit; every step of the construction must be detailed and explained thoroughly in ensure anyone can look it over and understand how to build the cockpit. Once the blueprint is made, construction of the cockpit should begin. Once the construction is over, more testing of the actual cockpit should occur, to make sure all the assumptions made by the design will still hold.

3.2 Drivetrain

3.2.1 Preliminary Work

At the beginning of the semester, the team decided that a major goal would be to build a test cart that would test the drivetrain and propulsion system. The basic concept behind this vehicle was to install the actual drivetrain and propulsion systems into a mockup cockpit on wheels. In this way the pilot could sit in the cockpit and pedal just as he would in the actual

plane. If the propeller spins at the required RPM without complication, it will be verified that the drivetrain can withstand required loads. To complete this goal, the drivetrain needed to be constructed. Previous HPA teams left behind a preliminary design which is pictured in Figure 3.2.1-1.

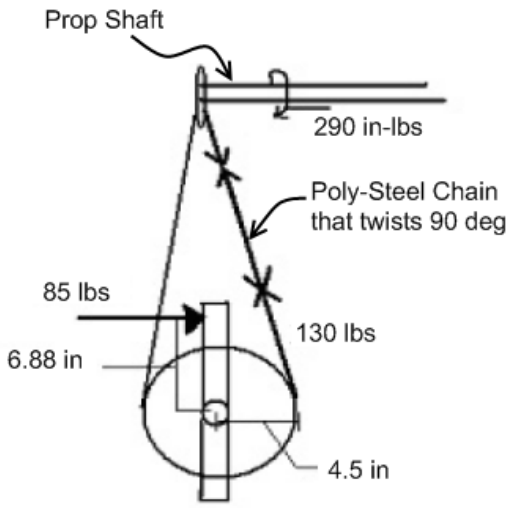

Figure 3.2.1-1 Preliminary drivetrain design left by past HPA Teams

After looking into ordering the parts described in this design, however, it was determined that the poly-steel chain that was called for was no longer in production. Other materials that could support 90^o of twist, such as belts, were researched thoroughly in an effort to keep the weight to a minimum. However, nothing was found that could work reliably at the design sprocket center distance, RPM, and belt/chain tension. Therefore, it was determined that the system had to be redesigned.

3.2.2 Drivetrain Redesign

After determining that the first drivetrain design was infeasible, several alternative concepts were explored. The selection factors that were given the most weight in the design selection process were simplicity of design (leading to lower weight) and simplicity of construction. The new design concept, pictured in Fig. 3.2.2-1, turned out to be very similar to the first design. This system is made from pre-fabricated bicycle parts and a pair of miter gears (bevel gears with a 1:1 gear ratio) to change the axis of rotation by 90^o.

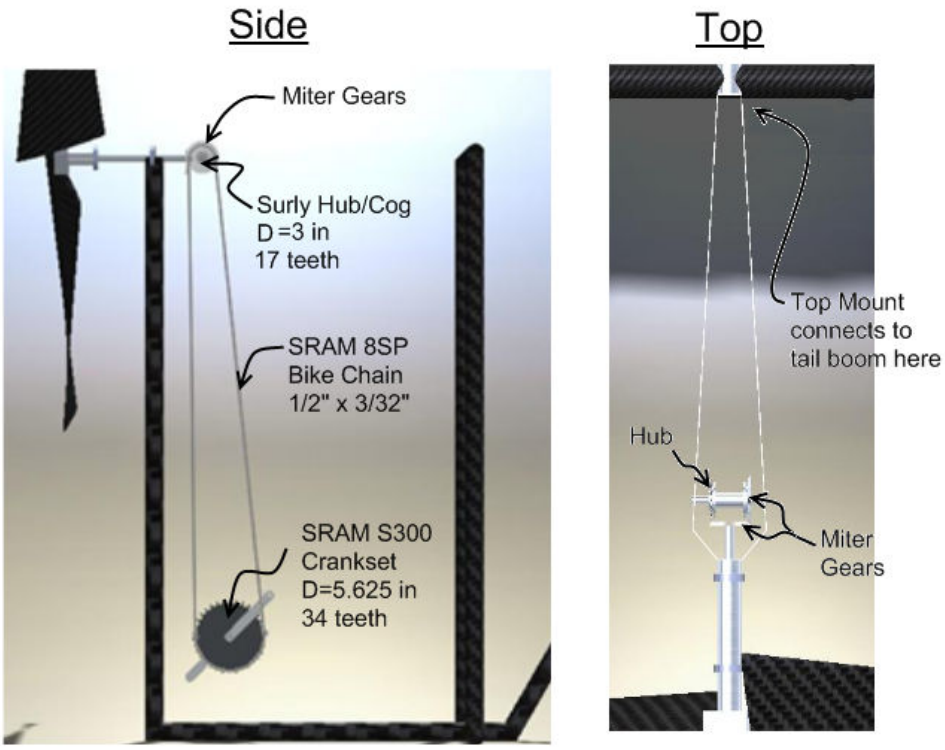

Figure 3.2.2-1:Current drivetrain design including possible hub to cockpit mounting system shown it the top view

This drivetrain system has many advantages over the old design. First, using bicycle parts greatly eases construction while simultaneously increasing reliability. Also, bicycle parts are capable of supporting loads much greater than are called for in our design. Finally, the bike parts used in construction turn out to be relatively light; having a design weight of only about 3.5 lbs not including the miter gears.

3.2.3 Drivetrain Components

3.2.3.1 Crank set

The crank set used is a SRAM S300 Crank set. This piece comes from production with two hard anodized coated chain rings; however, the larger one was removed for weight savings. The smaller chain ring has 34 teeth and a diameter of about 5.625 in. The crank arms are made of AL-6061-T6 Alloy and have a moment arm of 6.5 in. This set also comes with a bottom bracket for mounting and can be seen in Fig. 3.2.3.1-1. The total weight of this crank set is 1.752 lb.

Figure 3.2.3.1-1: SRAM S300 Crankset with bottom bracket shown top right

3.2.3.2 Chain

In the new drivetrain design, the mechanism used to transfer power from the pedals to the propeller shaft is the SRAM PC-890 Power Chain II. This chain, which can be seen in Fig. 3.2.3.2-1, is a lightweight 8-speed bicycle chain. The links are 1/2" x 3/32" and the total chain weighs 0.687 lb. and has a length of 4.75 feet. Because the exact center distance between the crank set and cog is not known at this point, two chains were purchased so that any chain length up to 9.5 feet is possible.

Figure 3.2.3.2-1: SRAM PC-890 Power Chain II bicycle chain to be used in current design

3.2.3.3 Hub/Cog

The sprocket that transfers power from the chain to the propeller shaft is called a cog. The cog used in the current design is a Surly threaded track cog, shown in Fig. 3.2.3.3-1.

Figure 3.2.3.3-1: Surly threaded track cog 17t x 3/32"

This cog is made from machined, heat-treated and chrome plated SCM415 CroMoly steel. It is about 3 in. in diameter and has 17 teeth, which gives the desired 2:1 gear ratio between the cog and the crank set with 34 teeth. The cog has a bore through the center that has a diameter of 1.375 in. and a standard ISO threading of 24 tpi, which allows it to simply screw onto the hub.

The mechanism that will transfer the rotation of the cog to the bevel gears is a bicycle rear hub, which is essentially the center of the rear wheel. This hub will also be used as the mechanism for mounting the cog and gear to the top of the cockpit. The specific hub used for this drivetrain is a Surly Rear Fix/Fix Track (120mm spacing or width) Hub which is pictured below in Fig. 3.2.3.3-2. This hub is made from forged aluminum with medium height flanges, and spins on high load, adjustable cartridge bearings over standard sized axles (10 x 1mm).

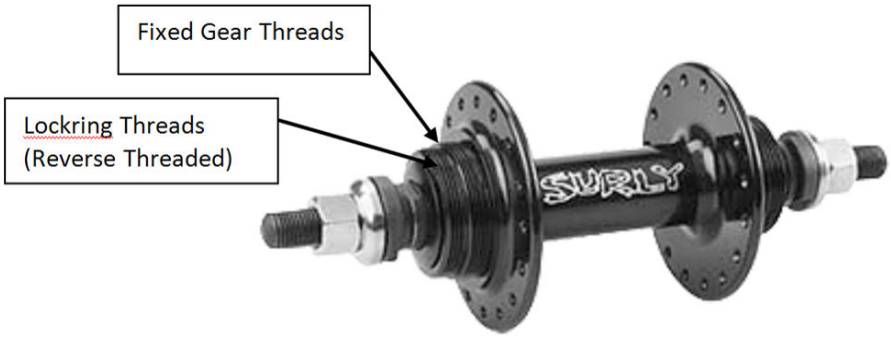

Figure 3.2.3.3-2: Surly Rear Fix/Fix Track Hub

This hub is essentially the simplest form of a rear wheel hub which gives it the lightest weight. The fixed gear configuration on both sides of the hub means that the freewheel has been eliminated, since it would be of no use in this application. Instead, both sides of the hub have fixed gear/lock ring threads (1.37 in. x 24tpi). In this way, the cog is screwed onto the hub and then a lock ring with reverse threading is screwed on to prevent the cog from slipping. The lock ring used also came from Surly and can be seen in Fig. 3.2.3.3-3. This part is made from CNC-machined stainless steel and has an inner bore that is 1.29 in. in diameter with a threading of 24tpi.

Figure 3.2.3.3-3: Surly lock ring used to secure the cog to the hub

Since the hub has the same configuration on non-cog side, a miter gear can be ordered with a 1.375 in. x 24tpi bore as well allowing for simple assembly. At this point, the miter gears are the only parts that are yet to be purchased. The gears will be explained in more depth in the next section. Figure 3.2.3.3-4 shows the parts that have been purchased

(hub, cog, and lock ring) assembled together. The total weight of the hub, cog, and lock ring is 0.848 lb.

Figure 3.2.3.3-4: Hub with cog and lockring mounted to it

3.2.3.4 Miter Gears

The parameters and constraints governing the design of this gear system are outlined in Fig. 3.2.3.4-1. Currently, the miter gears are in the process of being ordered from a website called rushgears.com that offers a variety of options in custom gear design. At the moment, sketches have been sent to the company for design verification and a price quote. The team remains hopeful that the design is quickly approved by the company and that the gears can be manufactured and installed on the test vehicle before the end of the semester.

Referring to Fig. 3.2.3.4-1, the main parameters that will constrain gear design will now be described. The first parameter for the gear design is that the center of the propeller shaft must align with the midpoint of the hub between the two flanges. This leads to the constraint that the diameter of both gears at the first point of contact must be 2 7/8 in. This also guarantees that the miter gears will clear the flanges. The second main constraint is that the miter gear attached to the propeller shaft must not run into the cog. This sets the maximum outer diameter for the gears at 3 3/8 in.

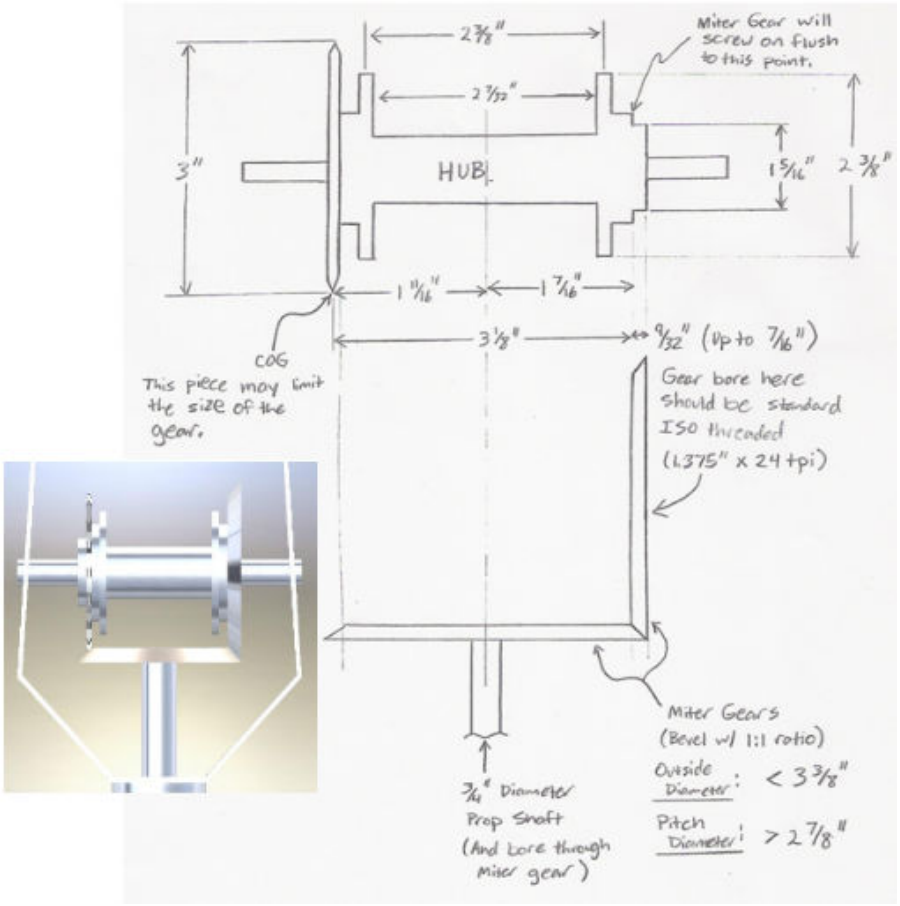

Figure 3.2.3.4-1: Current miter gear design concept (not to scale) along with CAD drawing

A final design consideration is that the gear attaching to the hub should have a hole bored that allows it to screw onto the hub. This requires the bore to have a diameter of 1.375 in. with standard ISO threading of 24tpi. Additionally, the gear must fit the hub thickness wise. Ideally, this gear would have the thickness of the fixed gear threading (9/32 in.) so that a lock ring could fit on its threading and secure the gear. However, this may be too small of a thickness. If the fixed gear thread thickness is too narrow, the gear could overlap the lock ring threading and set screws could be used to add additional resistance to slippage. This sets the maximum thickness of the hub miter gear at 7/16 in.

3.3 Wings

3.3.1 Main Wings

There have been no changes to the wing design this year.

3.4 Tail

3.4.1 Tail Wings

The tail wings geometry was fully designed last semester, though there was a mistake in the calculation. The mistake was that the aspect ratio was used instead of area in the table, which made horizontal tail relatively smaller than vertical tail. The correct final dimensions for the tail wings are shown in the Table 3.4.1-1 for both the horizontal and vertical tail. The tail wings are structured by spars, ribs and a skin, which are made of carbon fiber tubes, foam, and duralar skin respectively.

Table 3.4.1-1 Dimensions of tail wings

	Horizontal Tail	Vertical Tail
Ave. Chord(ft)	2	3.14
Max. Chord(ft)	2.86	4.49
Min. Chord(ft)	1.14	1.8
Span(ft)	14	7.5(upper) 3.5(lower)
Area(ft^2)	28	34.5
AR	7	3.5
TR	2.5	2.5

3.4.2 Ribs

The airfoil of the tail wings was decided to be the NACA0012 airfoil for its small drag coefficient and large maximum thickness for the spar to fit in. This airfoil allows the maximum diameter of spars to be 1.48 and 2.33 inches for the horizontal and vertical tail wings respectively, while having a drag coefficient of 0.0060 at 0 degree angle of attack. MATLAB code was written to calculate dimensions of each rib for desired number of rib. Our first design of the horizontal tail has 15 ribs, and the vertical tail has 7 ribs on the upper wing, one at the center, and 3 ribs on lower wing. Each rib is placed about 1 foot apart from each other. The thickness of each rib was designed to be 10% of the maximum thickness to keep the strength distributed over the wings. The spar position was placed on 30% of the

chord length where the maximum chord thickness exists to maximize the strength of the spar and load distribution on the spar. The detail dimensions for each rib were shown in Table 3.4.2-1 and 3.4.2-2 for horizontal and vertical tail respectively.

Table 3.4.2-1 Ribs dimensions for horizontal tail

Rib#	Chord Length(inch)	Spar position(inch)	Max Thickness(inch)	Rib Thickness(inch)
1	13.71	4.11	1.65	0.16
2	16.65	5.00	2.00	0.20
3	19.59	5.88	2.35	0.24
4	22.53	6.76	2.70	0.27
5	25.47	7.64	3.06	0.31
6	28.41	8.52	3.41	0.34
7	31.35	9.40	3.76	0.38
8	34.29	10.29	4.11	0.41
9	31.35	9.40	3.76	0.38
10	28.41	8.52	3.41	0.34
11	25.47	7.64	3.06	0.31
12	22.53	6.76	2.70	0.27
13	19.59	5.88	2.35	0.24
14	16.65	5.00	2.00	0.20
15	13.71	4.11	1.65	0.16

Space between ribs:	1 ft
Diameter of the spar:	1.37 inch

Table 3.4.2-2 Ribs dimensions for vertical tail

Rib#	Chord Length(inch)	Spar position(inch)	Max Thickness(inch)	Rib Thickness(inch)
1	21.55	6.47	2.59	0.26
2	26.17	7.85	3.14	0.31
3	30.79	9.24	3.69	0.37
4	35.41	10.62	4.25	0.42
5	40.02	12.01	4.80	0.48
6	44.64	13.39	5.36	0.54
7	49.26	14.78	5.91	0.59
8	53.88	16.16	6.47	0.65
9	43.10	12.93	5.17	0.52
10	32.33	9.70	3.88	0.39
11	21.55	6.47	2.59	0.26

Space between ribs (upper):	1.07 ft
Space between ribs (lower):	1.17 ft
Diameter of the spar:	2.12 in

3.4.3 Connector

The connectors between the tail boom and the tail wings not only attach the tail boom and the tail wings but also allow the tail wings to rotate at the spars. The first idea was to have external hinges. This hinge has one end attached to the tail boom and the other end attached to the wing. However, this will create a lot of weight and drag. The second idea was to have wire to fix the position. Even though this would save weight, this would be too unstable and too hard to implement on the control surfaces. Then the third idea was to use the tail boom as a part of the hinge. This is possible by taking a piece of metal plate and attaching one end of it to the tail boom with a bolt and the other end to the tail wing spar. This would be simple, light and creates less drag. The drawing is shown in Figure 3.4.3-1 and Figure 3.4.3-2, and dimensions are shown in Table 3.4.3-1. One plate design is weak for roll and yaw moment, and two plates design was suggested for better structure and the design still need to be finalized.

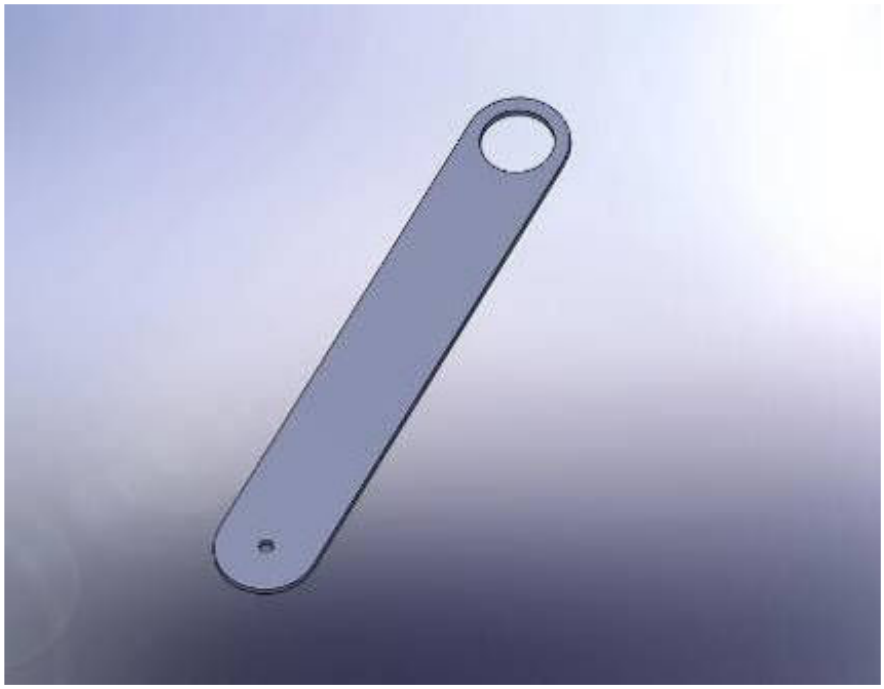

Figure 3.4.3-1: CAD drawing of Connector

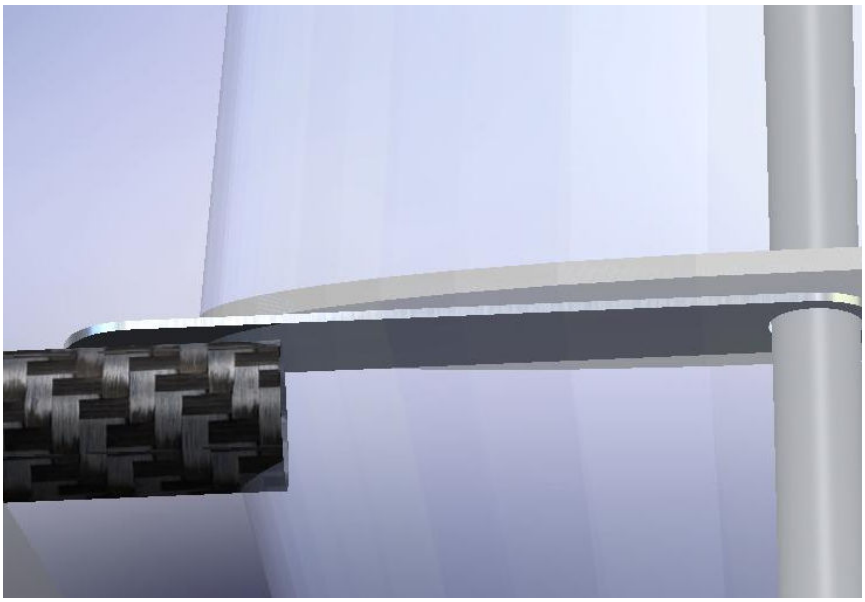

Figure 3.4.3-2: CAD drawing of Connector

Table 3.4.3-1 Ribs dimensions for connector

	Horizontal Tail	Vertical Tail
Length (in)	10.5	21.5
Width (in)	2.5	3.5
Thickness (in)	0.25	0.25

3.4.4 Control

Both tail wings are supposed to be able to rotate at each spar. The current design to rotate the tail wings is to use an electronic push box. However rotating the whole wing is expected to require a lot of power while flying due to lift and drag created by the tail wing. This calculation is uncertain and is still in progress. After finding the required power, the best push box will be chosen.

3.5 Weights

3.5.1 Weight Locations

Because of the necessary low weight for a human powered aircraft, the distribution of weights to different components must be carefully monitored. The joint and propeller weights are based on measurements taken from components constructed by previous teams. The

allotted weights versus the estimated weights of a few components are shown in Table 3.5.1-1.

Table 3.5.1: Current Mass Allowance

Component	Allowance (lb)	Estimate (lb)
Spars	15.3	9.64
Struts	2.40	2.08
Ribs and Skin	3.50	--
Joints	3.50	--
Tail Boom	21.7	--
Propeller	2.00	--
Drive Train	3.13	--
Cockpit Frame	5.00	3.40
Vertical Tail	7.88	--
Horizontal Tail	7.22	--
Empty Weight	71.63	--
Pilot	140	140
Total Weight	215	--

This table is not complete, but does represent the major components of the aircraft, minus the elevator and rudders spars. The component weights table will be updated as structural members are constructed to reflect actual weights; specifically, the propeller and wing ribs can both currently be weighed. To allow room for uncertainty, the allowed weights do not necessarily add up exactly to the total allowed weight. For the 2008-2009 Team, some of the weight estimates have been restored from the 2006-2007 Team's estimates to allow for three significant digits instead of two [5]. The estimated weights for the cockpit frame, wing spars, and wing struts are currently under their weight allowance.

As components are in the process of being finalized, the CG estimate of the entire aircraft must be considered. It is especially important that future teams understand how the CG varies between when the aircraft is empty and when the aircraft has a pilot. Without a pilot, the CG location will not be properly balance, and great care must be taken to make sure that the front and top heavy aircraft does not tip over. Tipping could cause the propeller to be broken.

Currently, only the weights of the wing struts and spars are estimated exactly, although they are subject to change. However, it was possible to create a program using "dummy values" for other components not completely designed as of yet. As dummy values are being used, an example table of the CGs will not be provided at this time. An example of the program's output can be seen in Figures 3.5.1 - 3.5.3. Code (CG_totSolving.m) is in Section 10's program listings.

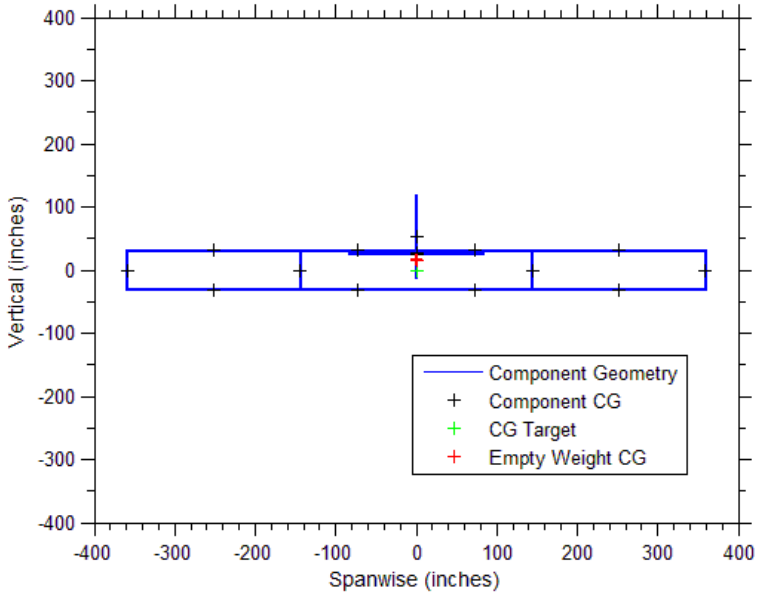

Figure 3.5.1: CG_{tot} Estimate of Various Components, Front View

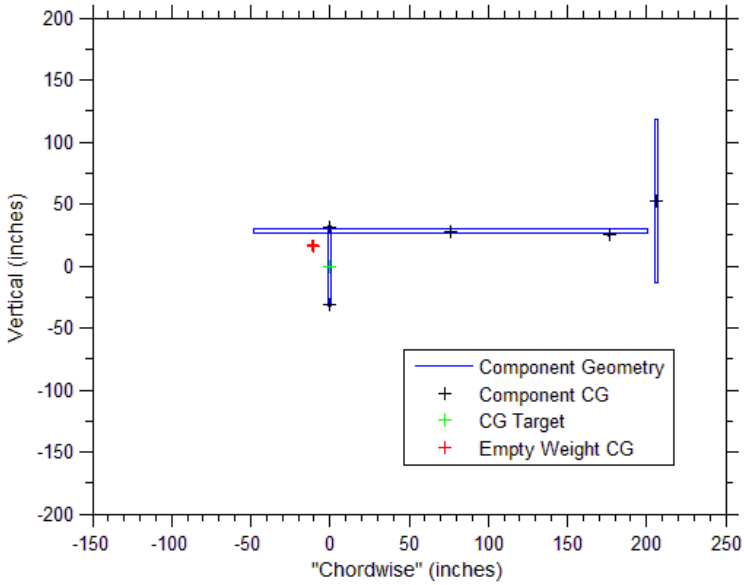

Figure 3.5.2: CG_{tot} Estimate of Various Components, Side View

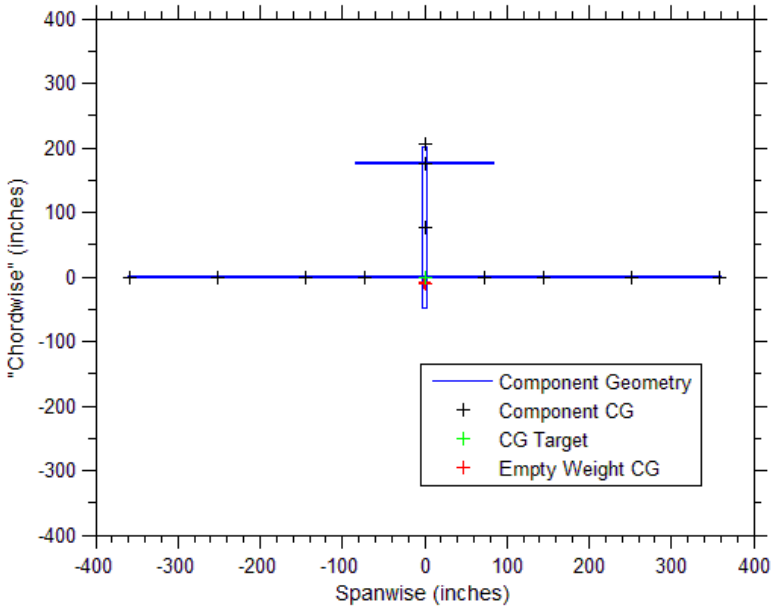

Figure 3.5.3: CG_{tot} Estimate of Various Components, Top View

The components being modeled are the wing spars and struts, the tail boom, the propeller (not shown), and both the horizontal and vertical tails. Each component's CG is noted with a black marker, while CG_{tot} is designated with the red marker. The center of the wings has a green marker; this location is noted because it is important for CG_{tot} to be in the middle of the wings for control purposes (only when considering the front view). Failing to keep the CG in the middle of the airfoils will lead to undesirable moments on the aircraft. However, the location might not be the exact desirable location, and will possibly have to be moved.

This program first begins with the general properties and dimensions of each part, including their materials. Afterwards, it computes first the part weights, then the CGs of the parts with respect to themselves. The CGs are then translated to the reference point corresponding to "center" of the wings as seen from the front of the aircraft. The parts are then drawn, followed by their respective CGs, and then the estimated CG_{tot} of the aircraft. By drawing the parts of the aircraft onto a plot, it is possible to "eyeball" the results for accuracy while understanding the configuration of the aircraft.

The shown rough estimate does not include the pilot, whose location will greatly affect the final CG_{tot} of the aircraft, but it was discussed in the final report for the 2006-2007 Team [5]. Also not shown are the ribs for the wing and tails, as they weigh much less than the struts and spars, at approximately 0.006613 lbs (3 grams) each, according to estimates by previous teams. It will be necessary to add the weights for the joints, drive train, coverings or skins, and other miscellaneous hardware in order to get the closest estimate possible of the aircraft's CG_{tot}. It may also be necessary to update the V-n diagram used in previous years' reports as well as prepare a proper mission profile. Finally, parts may need to be moved to their proper locations as the geometry of the aircraft is refined.

Future work mentioned in the previous paragraph has partially been left as an exercise for future teams. The program is ready to compute where the pilot should be located as well as adding the cockpit to the diagrams. Also available, in the 2005-2006 Team's final report, are the CG locations of the RC model of the aircraft [4].

4. Prototype Construction

4.1 Cockpit

4.1.1 Dimensions

As shown in figures 4.1.1-1 and 4.1.1-2 below, the cockpit frame is constructed of 2 inch diameter carbon fiber tubes. The frame consists of a top bar which supports the tail boom and propeller, a front bar which defines the leading edge of the airfoil, a back bar that slants upward at a 30 degree angle from vertical, a bottom bar which connects the front and back, and two side bars which act as supports for the wings.

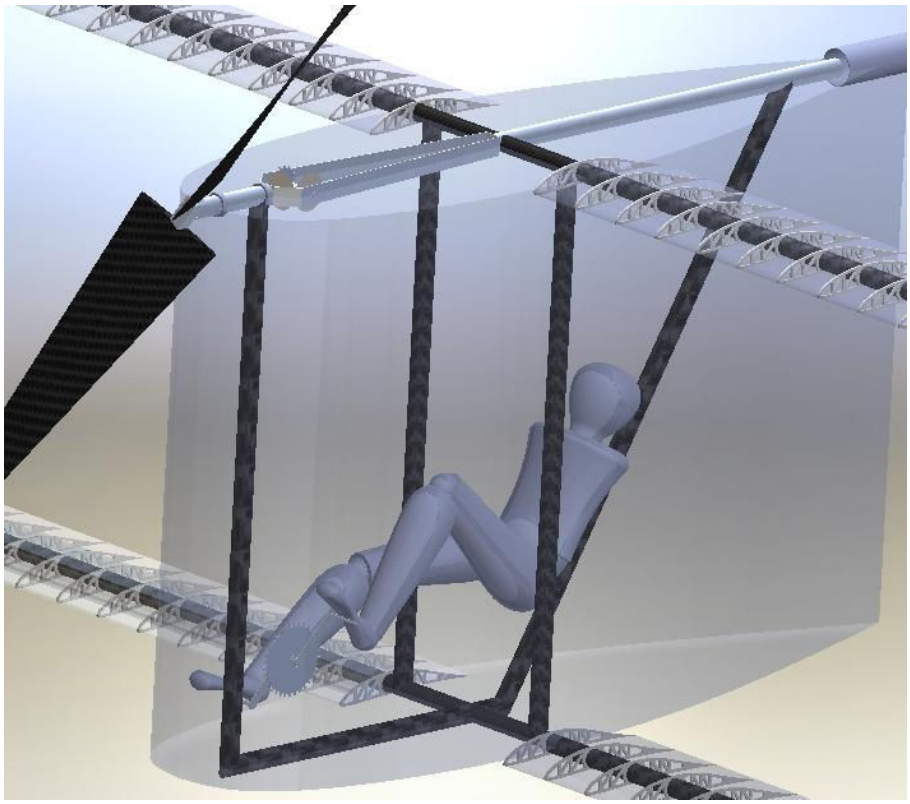

Figure 4.1.1-1: Three dimensional view of cockpit

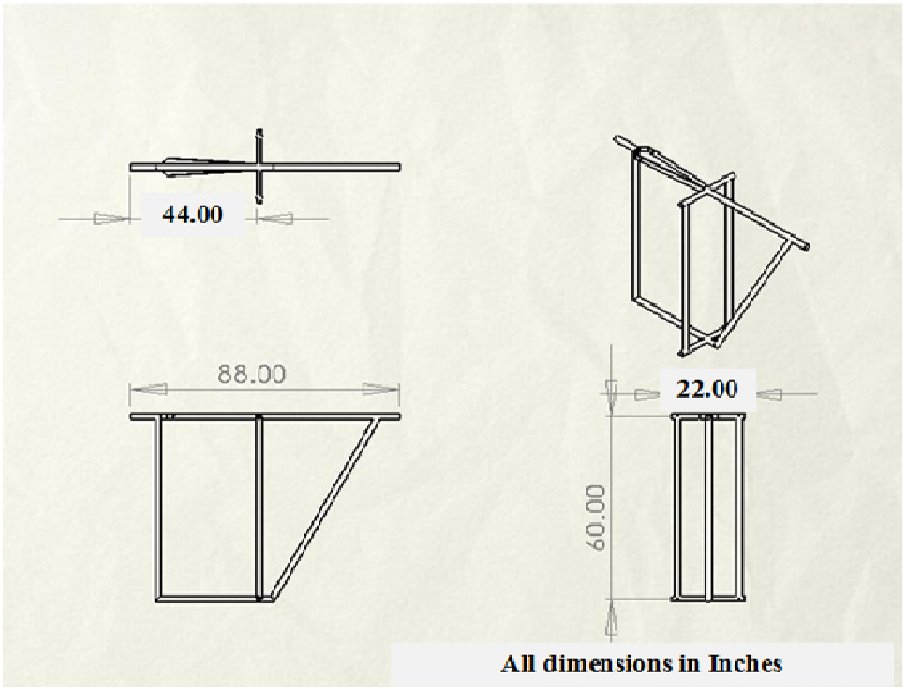

Figure 4.1.1-2: Construction drawing for cockpit frame

The chosen airfoil is a Van De Voren with 17% thickness and a 44 degree trailing edge. The pilot is seated in a recumbent position with the seat mounted to the back bar of the cockpit. The pedals should be located between 33 and 42 inches from the seat and the seat must be adjustable to allow for different pilots. In addition, a 30 degree angle between the pedals and seat and the horizontal bar has been determined to be the optimal angle to allow the pilot to pedal most efficiently.

4.1.2 Construction

The tubes for the cockpit frame will be purchased from a carbon fiber manufacturer to ensure high quality. Joints are either formed of carbon fiber or lashed with epoxy soaked Kevlar. Seat position has yet to be determined, but will be based on the airfoil selected to enclose the cockpit. The skin of the cockpit will be formed of duralar wrapped around a wire and nylon string form. The wire will be bent into the appropriate airfoil and attached to the top bar and bottom bar of the cockpit frame. Nylon string will be run between the two wire airfoils to provide a structure for the duralar which will be wrapped and sealed after the pilot is in position.

4.1.3 Mock Cockpit v2.0

With a new cockpit design, it became necessary to build a new mock cockpit. The new mock cockpit, as shown in Figure 4.1.3 is made of PVC pipe, the same material as used in the previous mock cockpit [6]. The PVC pipe used has a diameter of 2 inches, and is built almost exactly as the real cockpit would be built. The only part of the mock cockpit's design that is not exactly how it would be built is the back bar. The real cockpit would have a straight bar angled at roughly 36^{o}. This angle is not possible to create using PVC pipe, so some adjustments were needed on this area.

Figure 4.1.3: Mock Cockpit v2.0

4.2 Drive Train

4.2.1 Dimensions

As shown in figures 4.1.1-1 and 4.1.1-2 below, the bicycle gears for the drive train are in a 2 to 1 ratio, allowing the pilot to pedal at 90 rpm and turn the prop at the optimal 180 rpm. The bicycle gears are high-quality racing gears purchased from a local bike store. The bevel gears will need to be special ordered to have a bore diameter of 0.75 inches to match the diameter of the drive shaft and threads which match the gear hub. The pedal-crank assembly will be located 10 inches vertically from the bottom bar of the cockpit and 12 inches aft of the front bar. It will be attached to the cockpit frame using aluminum brackets modified from a racing bike.

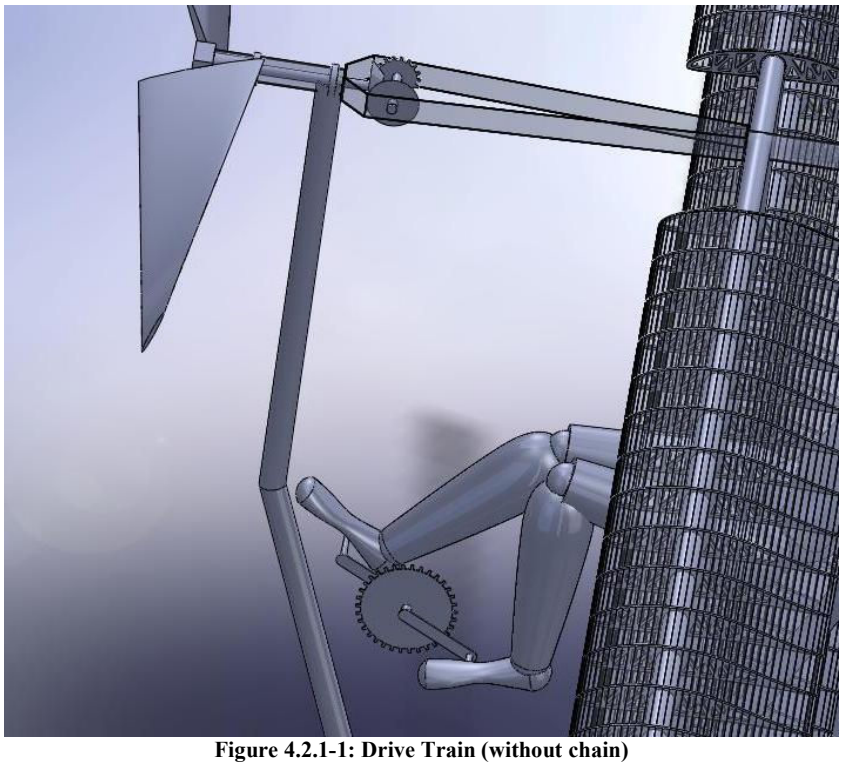

Figure 4.2.1-1: Drive Train (without chain)

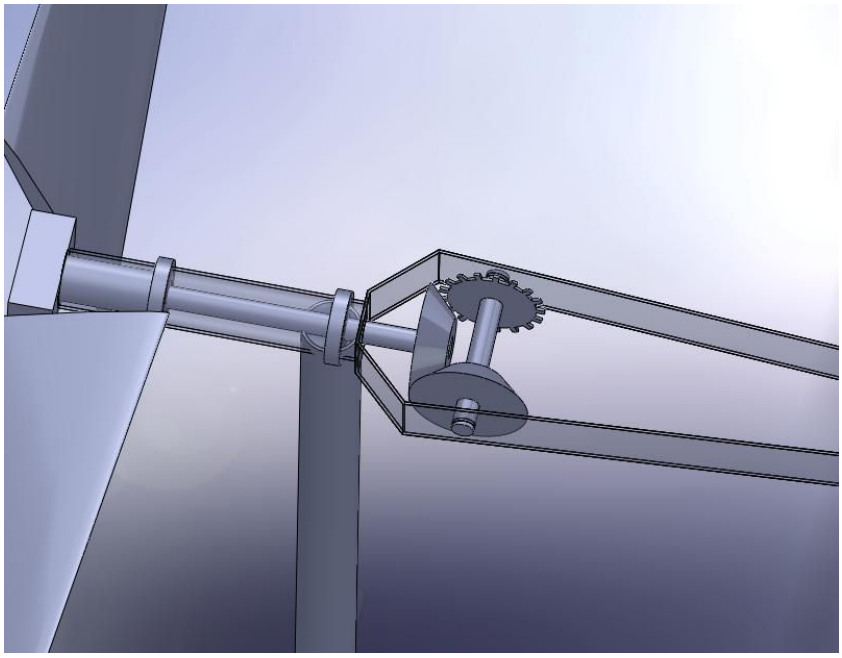

Figure 4.2.1-2: Gear Hub (without chain)

4.2.2 Construction

The drive train consists of a bicycle crank attached by a gear to a modified bicycle hub to which a bevel gear has been attached. The bevel gear mates to a bevel gear attached to the drive shaft. It has been recommended, based on other HPA designs, that the bevel gears

be constructed of steel to prevent shearing problems. The modified bicycle hub is supported by modifying the top bar to include a pair of aluminum bars to which the hub can be bolted. The length of these supporting aluminum bars has not been determined.

The hub and bicycle parts have been purchased. The larger gear is mounted to the cockpit frame by standard bicycle components, and the smaller gear hub is mounted between the aluminum support bars incorporated into the upper frame of the cockpit. A standard bicycle chain runs between the lower and upper sprockets.

The drive shaft is connected to the propeller by a specially constructed aluminum fitting which is currently attached to the dynamometer. The drive shaft is supported within the upper tube of the cockpit frame by thrust bearings which are held in place by rings with set-screws attached to the drive shaft which prevent the drive shaft from sliding forward or backward. A bracket should be added between the front bar of the cockpit and the upper bar which extends forward to support the weight of the propeller.

4.3 Wing

4.3.1 Dimensions

As shown in figures 4.3.1-1 through 4.3.1-4, the wing of the HPA has a span of 60 feet, broken into eight 9 foot sections and two 12 foot section per wing.

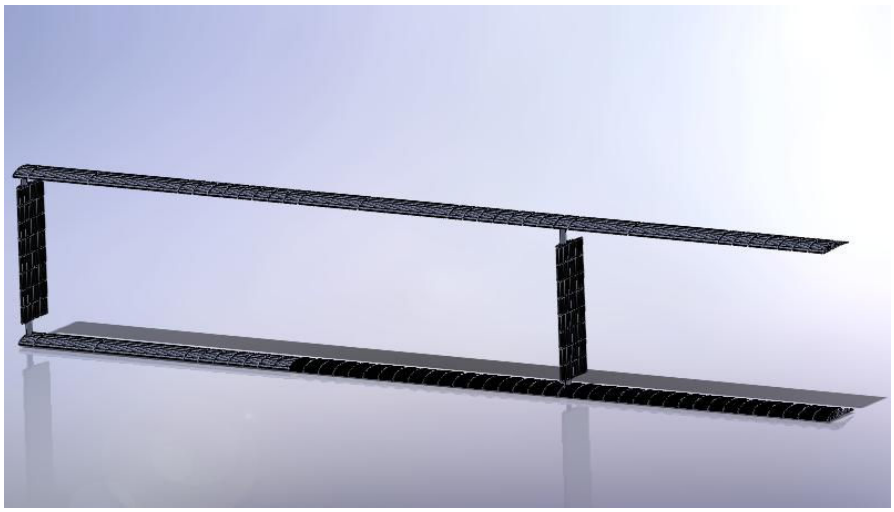

Figure 4.3.1-1: Left Wing

A supportive strut is located at the end of the span as well as 18 feet inboard from the end of the span at the joint between the 12 foot and 9 foot sections. The 12 foot sections have a 2 inch diameter spar and a DAE-11 airfoil while the 9 foot sections have a 1.75 inch diameter spar and a DAE-21 airfoil. The two wings of the box-wing design are arranged in the same plane vertically with the spars 5 feet apart. The initial angle of attack for the wing has not been determined. The airfoil for the strut has not been determined.

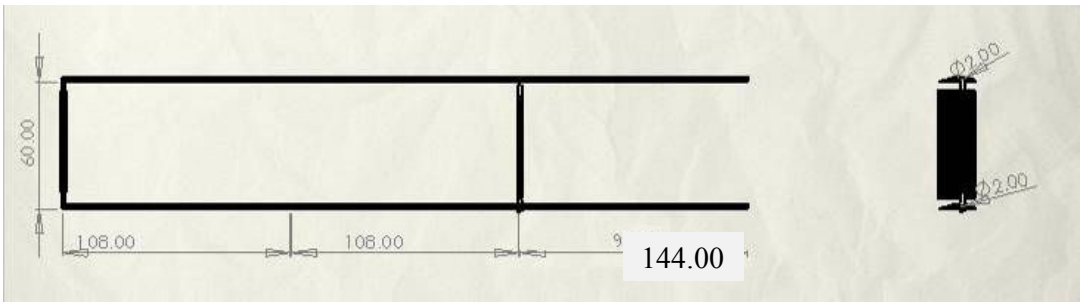

Figure 4.3.1-2: Left Wing assembly drawing

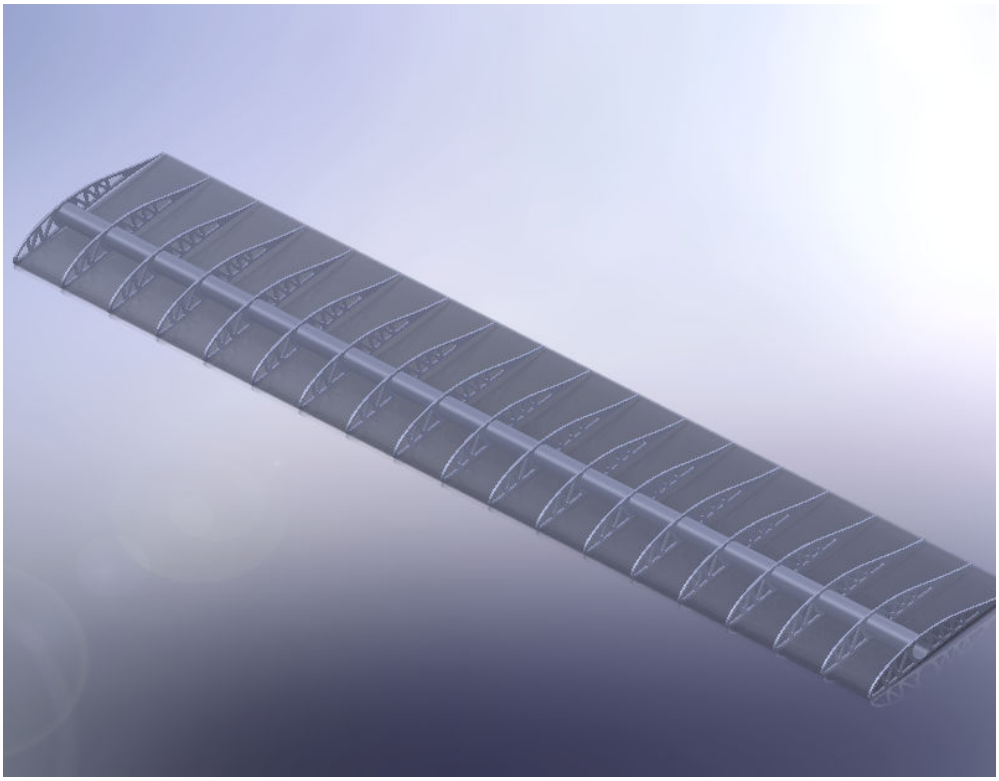

Figure 4.3.1-3: Nine Foot Wing Section

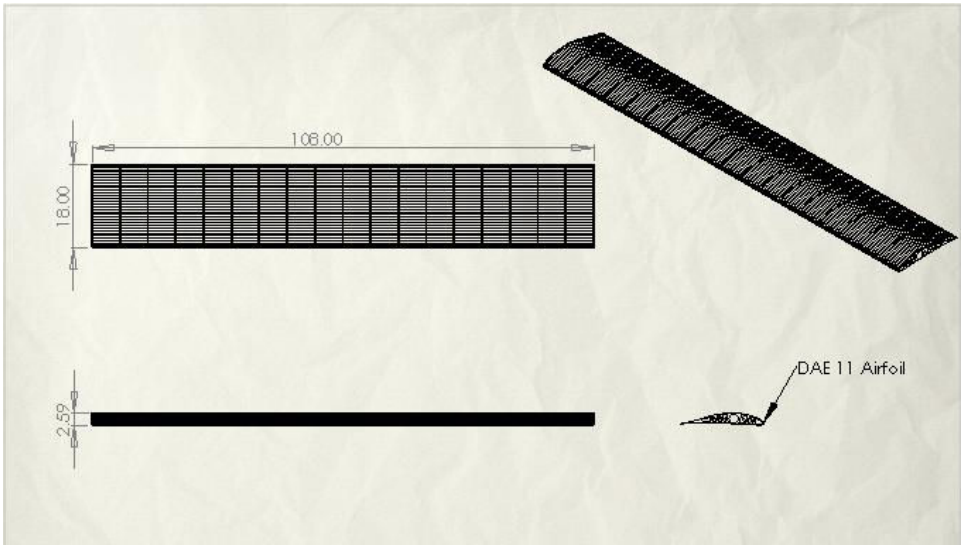

Figure 4.3.1-4: Nine Foot Wing Section assembly drawing

The spar is to be constructed from either 2 inch diameter carbon fiber or 2 inch diameter aluminum for the interior 12 feet of the wing, and 1.75 inch diameter carbon fiber for the outer 18 feet of the wing. The carbon fiber can be purchased pre-formed in 5 foot lengths which are joined together by inserting a smaller diameter carbon fiber tube at the joint. The struts are to be constructed of 1.75 inch diameter carbon fiber. Ribs of expanded Styrofoam with balsa leading and trailing edges define the airfoil's shape. Each rib is 0.25 inches thick and they are located every 6 inches on center for the wing.

4.3.2 Ailerons

Roll control is provided by ailerons located on the outer 18 feet of the two bottom wings. The ailerons are created by altering the original rib design. Figure 4.3.2-1 shows the cross section of an aileron rib. The ailerons are created separately from the airfoil and wrapped in duralar before being attached to the wing by packing tape. Aileron control will be achieved by use of electronic push-boxes located every 3.6 feet along the outer 18 feet of the lower wing spar.

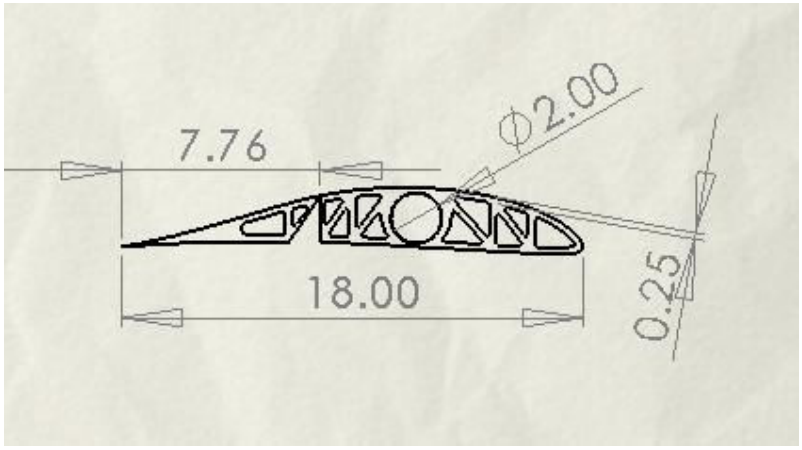

Figure 4.3.2-1: Aileron rib cross section construction drawing

4.3.3 Construction

Ribs are constructed by cutting the Styrofoam into airfoil shaped blocks which are then cut using aluminum templates as guides to remove excess material. The block is then cut into 0.25inch thick ribs. A piece of balsa is then glued to the top and bottom of each rib. The ribs are assembled on the spar and glued into place with a dab of epoxy. Once all of the ribs are on the spar, a leading edge of balsa is formed into a leading edge using the wooden molds located in the ware-lab. The leading edge is glued to the ribs and a trailing edge made of balsa is attached to each rib. Once the leading and trailing edges are in place, the entire wing is wrapped in duralar and the skin is shrunk into place with heat guns.

For the ailerons, the control surface is constructed separate from the wing and then attached with clear packing tape. The actuators are attached to the spar by balsa supports, and the push-rods extend through slots cut in the duralar skin between the wing and the control surface.

The struts consist of carbon fiber spars with foam and balsa ribs. They are constructed in the same manor as the wings. The struts are attached to the upper and lower wing spars via T and L joints formed of carbon fiber. These joints have already been constructed by previous year's teams.

4.4 Tail

4.4.1 Dimensions

The horizontal tail has a span of 14 feet with a maximum chord of 34.29 inches located at the center of the span, and a minimum chord of 13.71 inches located at the ends of the span. The vertical tail has a span of 11 feet with the maximum chord of 53.88 inches located 41.68 inches from the bottom edge and the minimum chord of 21.55 inches located at the top and bottom of the tail. The ribs are located every 13.04 inches on center along the 2.33 inch diameter spar. The airfoil for both the horizontal and vertical tails is a NACA 0012.

The horizontal and vertical tail are attached to a 4 inch diameter tail boom constructed of carbon fiber. One 8 foot section has been constructed by previous year's teams. The tail boom is 16 feet long, with the horizontal tail's spar located 13'6" from the front plane of the tail boom and the vertical tail's leading edge aligned with the back plane of the tail boom. The tail boom and tail-wing assembly is shown in figures 4.4.1-1 through 4.4.1-5.

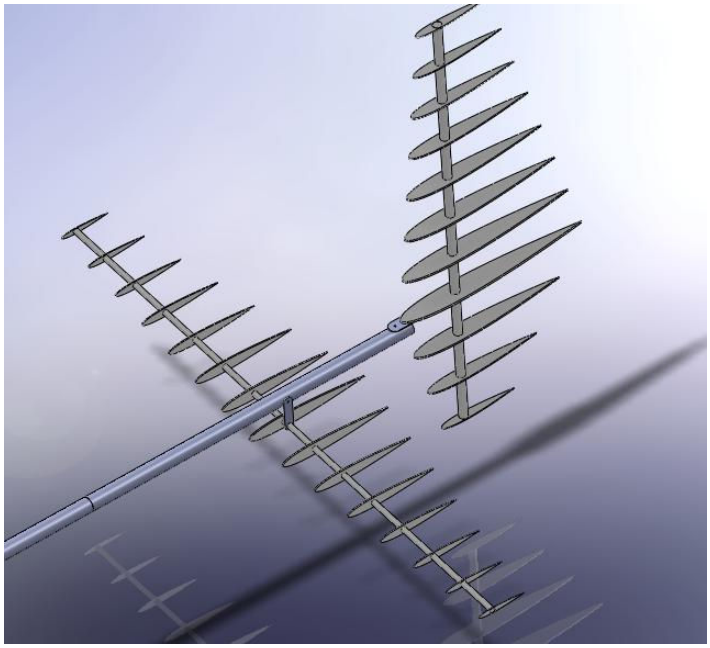

Figure 4.4.1-1: Tail Assembly (without skin)

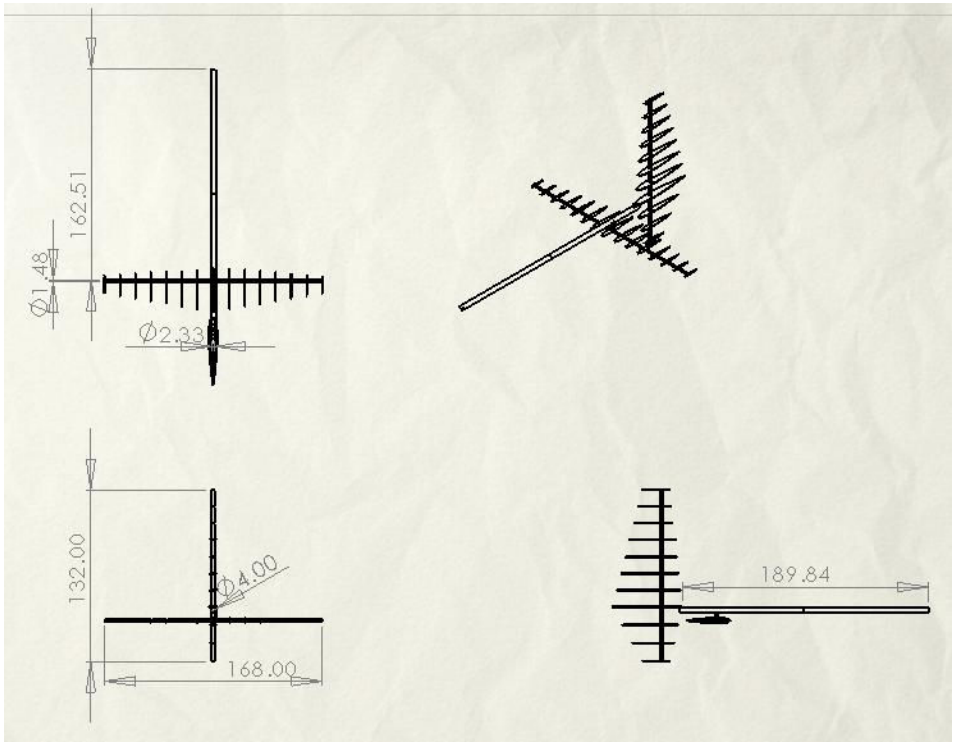

Figure 4.4.1-2: Tail assembly drawing

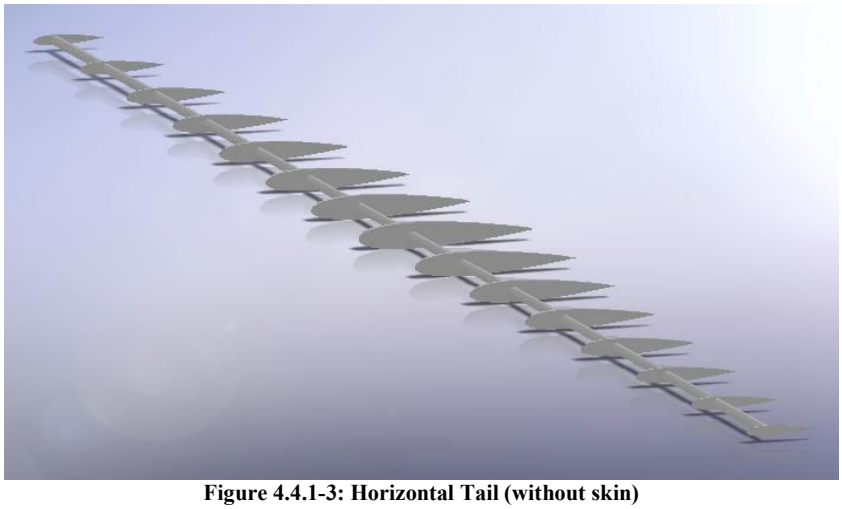

Figure 4.4.1-3: Horizontal Tail (without skin)

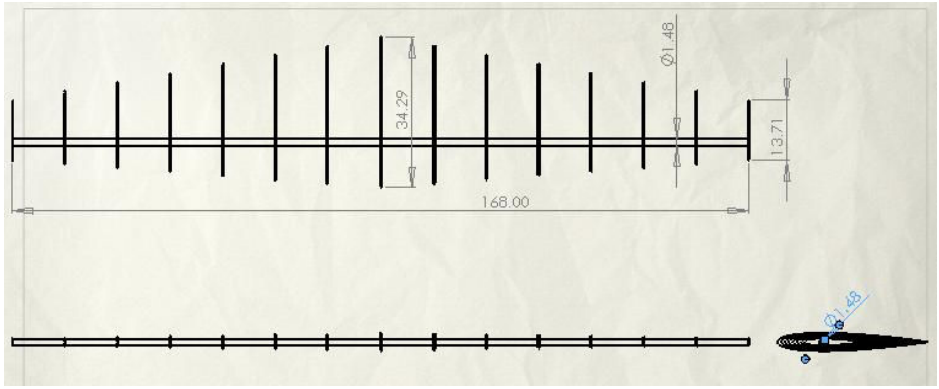

Figure 4.4.1-4: Horizontal Tail assembly drawing

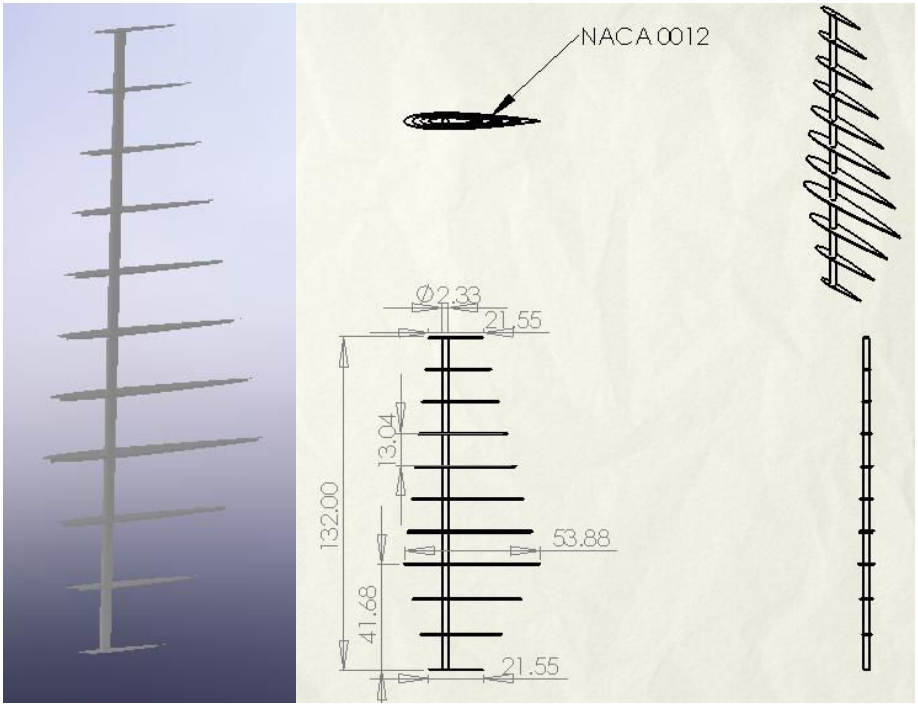

Figure 4.4.1-5: Vertical Tail 3-D and construction drawings (skin hidden for clarity)

4.4.2 Construction

The spar is carbon fiber and was purchased from a professional manufacturer to ensure minimum weight while maintaining high strength. Each spar is composed of 3 sections connected with other carbon fiber tube that is a little bigger or smaller. Templates for construction of the ribs has been made shown in Figure 4.4.2-1 and Figure 4.4.2-2 for horizontal and vertical tail respectively. The ribs are constructed in the same manner as the ribs for the wing, using foam and balsa. The leading and trailing edges will also be made of balsa, and the tail will be wrapped in duralar. All of the ribs for horizontal tail were cut out from foams shown in Figure 4.4.2-3 and tested to place them on the carbon fiber spar shown in Figure 4.4.2-4. The horizontal and vertical tails are connected to the boom by means of aluminum plates which attach directly to the carbon fiber tail boom by bolts. The spars are free to rotate and the entire tail surface acts as a rudder or elevator. The tail boom will be attached to the cockpit via lashing with epoxy soaked Kevlar.

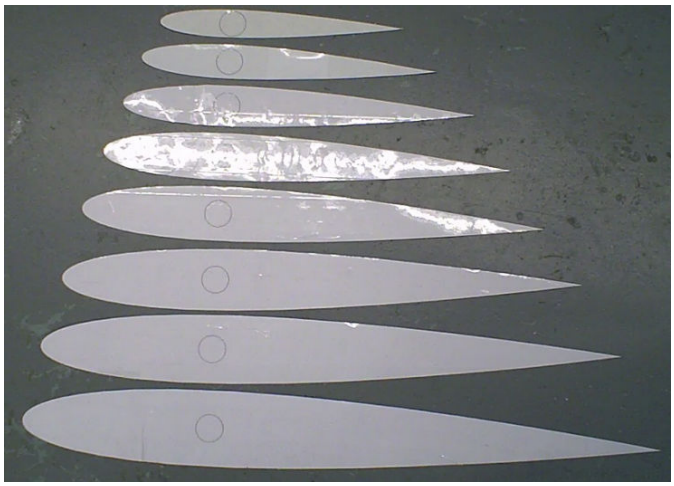

Figure 4.4.2-1: Template of horizontal tail wing ribs

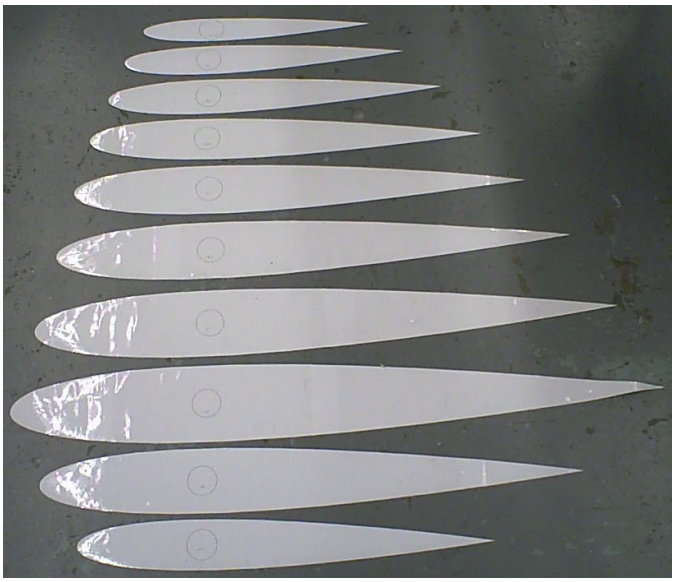

Figure 4.4.2-2: Templates of vertical tail wing ribs

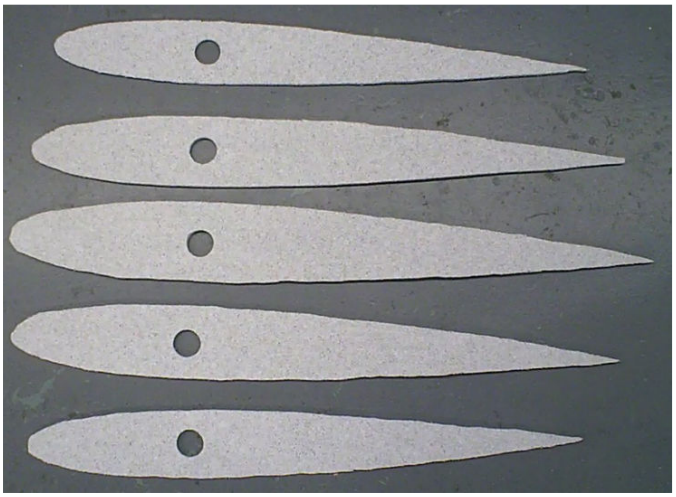

Figure 4.4.2-3: Ribs for horizontal tail wing

Figure 4.4.2-4: Horizontal tail wing

5. Testing

5.1 Cockpit Testing

The only testing done with the cockpit this year was test done to prove that an airfoil-like shape can be made around the cockpit's framework and that a human can actually fit inside this airfoil shape. As can be seen in Figure 5.1-1, the test was done inside the Human Powered Airplane team's spot in the W.A.R.E lab. The test used the mock cockpit constructed by one of the previous teams as the cockpit [6], used saran wrap to act as the material of the airfoil, and used string attached to the top and bottom of the cockpit to act as ribs for the airfoil shape.

Overall the test can be viewed as a partial success; we were able to wrap a human pilot, Mark Hollinshead, inside the cockpit, as shown in Figure 5.1-2. Our pilot was not very comfortable inside the cockpit, which was mainly because the airfoil shape made was an arbitrary shape and not the real airfoil shape. This test did show us that the proposed idea of creating the ribcage with carefully placed planks on the top and bottom of the cockpit, with string attached the ends is most likely not the way to go. Another team member, Kristen Moore, suggested the idea of using a stiff but light wire bent into the shape of the airfoil, and place this wire at the top and bottom of the cockpit. Once the wires are in place, it will then

be possible to carefully attach more lightweight wire to the top and bottom and create the airfoil shape that way.

The test was not able to determine if the current idea of getting the pilot into the cockpit and sealing him/her up afterwards will actually work. The current idea is to seal up one side of the cockpit first and leave the other side open. Then two or more people will pick up the pilot and side him/her through the cockpit. Once the pilot is inside the cockpit, the people holding the pilot must carefully position the pilot's feet and backside onto the pedals and the seat respectively, and try to have the pilot touch the pedals and the seat at the same time. Once the pilot is seated, one team member will begin attaching the wires to the airfoil shape, and a second team member will strap the pilot into his/her seat with our seat belt system, while the rest of the team will begin wrapping the rest of the cockpit up with the Dura-lar.

Figure 5.1-1: Airfoil testing

Figure 5.1-2: Mark wrapped inside the cockpit

5.2 Drivetrain

5.2.1 Propulsion Testing

5.2.1.1 Propeller Testing Overview

The propeller efficiency is a very important aspect of the propulsion system. To determine this propeller efficiency, η_p, the ratio output power to the input power is computed. Equation 5.2.1.1-1 from the 2007-2008 report shows this ratio.

$$\eta_p = P_{out}/P_{in} \quad (5.2.1.1\text{-}1)$$

The power output, P_{out}, is computed by multiplying the free stream velocity, V_0, by the thrust produced by the propeller, T. Equation 5.2.1.1-2 from the 2007-2008 report shows this.

$$P_{out} = V_0 * T \quad (5.2.1.1\text{-}2)$$

The input power, P_{in}, is computed by multiplying the input torque, Q, by the input shaft RPM, ω. Equation 5.2.1.1-3 also from the 2007-2008 report shows this relationship.

$$P_{in} = Q * \omega \quad (5.2.1.1\text{-}3)$$

To test the prototype propeller designed and built by previous year's teams, a dynamometer (dyno) was built and tested by the 2007-2008 team [6]. This dyno measures the values described above, allowing the efficiency to be determined. Since dynamic testing is needed to determine the effectiveness of the current propeller design, previous year's teams built a test cart designed to create a dynamic testing environment. It would be best to dynamically test the propeller in a wind tunnel, but propeller is too large for any wind tunnel the team has access to. The solve this problem, the dyno can be mounted to front of this test cart and pulled at the cruise speed of the airplane. Due to time restraints and multiple design problems with the dyno, the previous teams were only able to dynamically test the propeller once at a 0^o pitch angle and at only at 120 RPM. This test did not return any usable data except for displaying the problem areas with the test setup. The goal of this year's team was to fix the problem areas of the setup, and complete propeller testing dynamically.

5.2.1.2 Test Setup Problem Areas and Solutions

There were multiple problem areas with the previous team's dynamic propeller testing setup. These problems led to a lot of time and research for a solution for the current team. These areas included problems with getting measurements on the dyno as well as the method of moving the propeller at the cruise speed for dynamic testing. Each problem area and this year's team's solutions are discussed below.

The first hurdle for this year's team was the fix the dyno. The largest, most difficult and broad problem was that during the previous year's team's one test, there was no thrust reading from the propeller. This issue was studied and it was decided it could be due to a number of different aspects of the dyno. The first reasoning for the problem was that there was no force being read due to the inertial forces acting on the set up. The dyno motor, the chain drive system, propeller, and propeller shaft are all mounted on the free moving part of the dyno. This is a heavy load, and the idea was that the inertial force on the free moving section of the dyno from the test cart being accelerated was too much for the propeller to overcome. The test was done at a constant tow vehicle velocity, which was supposed to eliminate any inertial loading problems. When doing the test, it was noticed that there was always a little acceleration of the test vehicle because it was being pulled a rope behind a tow vehicle. The small elastic properties to the 300 ft rope causes these small accelerations, thus bringing inertial loading back into the system. Figure 5.2.1.2-1 given in the 2007-2008 report as Figure 5.3.7-1 shown below explains this inertial loading problem [6].

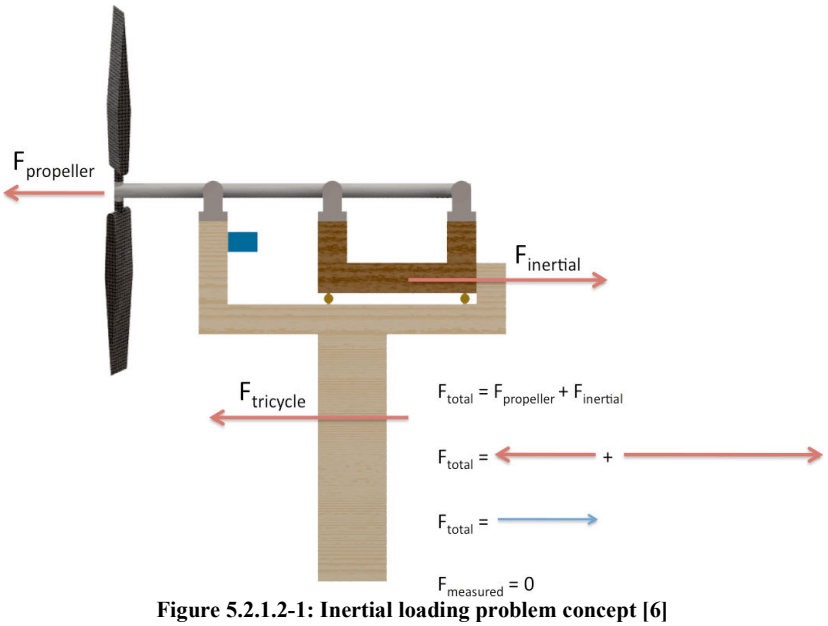

Figure 5.2.1.2-1: Inertial loading problem concept [6]

Adding to the inertial loading force to be overcome, the small friction in the sliders on the dyno may have made the inertial forces too large. Another potential reason for not getting a force reading is that one of the aluminum shafts in the motor gearbox powering the propeller was bent during the calibration of the torque load cell, and therefore the gearbox was not able to spin the propeller higher than 120 RPM. The design RPM is 180. This low RPM would produce a much lower thrust than the designed 5.5 lbs, another reason why the propeller could not move the free moving section of the dyno. The bent aluminum shaft is shown below in Figure 5.2.1.2-2.

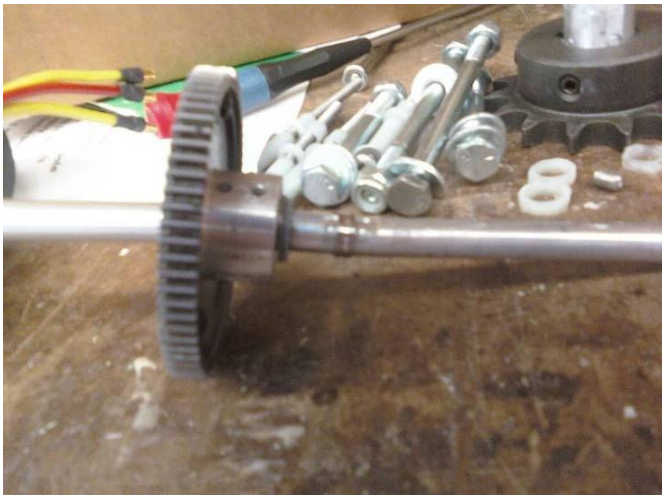

Figure 5.2.1.2-2: Bent aluminum dyno gearbox shaft

The second option for the problem with the dyno was the load cell used to measure the thrust was not sensitive enough to measure the small load of less than 5.5 lbs the propeller is supposed to produce at the RPM that was tested. The load cell that was being used was very inexpensive and purchased with very little background information on it. Thirdly, the problem may have been that at the lower than design RPM, the 0^o pitch angle that was tested did not produce any or enough thrust to produce a thrust reading on the load cell. This could be determined by testing at multiple pitch angles, but there was no time for this. Finally and most undesirably, the reasoning behind the dyno problems could be that the propeller just didn't perform to its design.

This year's team decided to disregard the final reasoning behind the dyno problems and assume that the propeller did produce enough thrust to be tested. Therefore the mechanical problems with the dyno needed to be fixed. After talking with previous team members, the current team decided to first fix the bent gearbox shaft as well as replace the thrust load cell and see if the problems were resolved. To replace the bent shaft, a steel shaft was purchased and machined to fit the setup of the gear box. For this replacement to be made, the entire dyno and gearbox needed to be taken apart. Figure 5.2.1.2-3 shows the new steel shaft with its inner gear mounted to it.

Figure 5.2.1.2-3: New steel dyno gearbox shaft

The team then purchased the new thrust load cell and it was installed as the dyno was put back together after the gearbox shaft replacement. The new load cell is a Measurement Specialties, Inc. FX-1901-10 load cell. It is rated for 0 -10 lbs of force and fits perfectly into the electrical set up currently installed on the dyno. This year's team took a lot of time to learn this electrical system and it's specifics to install this cell and get the dyno in a running condition. Figure 5.2.1.2-4 shows the new FX-1901-10 cell.

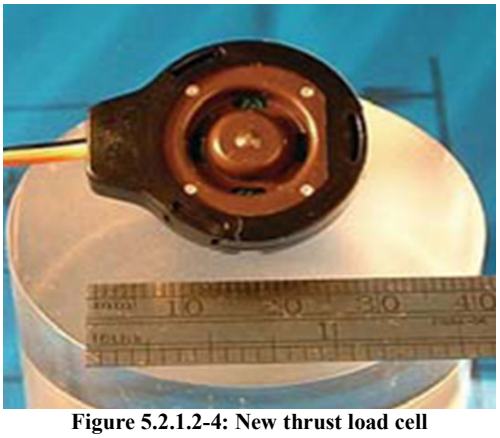

Figure 5.2.1.2-4: New thrust load cell

The team also added a third battery to power the propeller motor to the dyno system. This was in order to make sure the motor had enough power to spin the propeller at the design RPM of 180. It was noticed that with the previous set up of two batteries in parallel could only spin the prop at right around 120 RPM. After these upgrades to the dyno were made, the team began to calibrate the system with the goal of performing static thrust tests to verify the dyno was working properly before any dynamic testing could be done. During the calibration new problems were noticed. In order to use LabView 8.2 to measure the voltages output by the load cells, the signal coming from the cells must be amplified to a signal that the Natural Instruments NI-6009 Data Acquisition box can read accurately. When calibrating the new system set up, it was determined that the signal of torque load cell needed to be amplified more to fit into the range of forces that were being applied to the cell. This is an easy but time consuming fix, as different resistors need to be fitted into the amplification process in a trial and error method to fit the voltages for this set up. This new problem has not

yet been done yet, seeing as this torque reading only applies to dynamic testing. More time has been spent on a more important and pertinent to static testing and dynamic testing problem determined while calibrating the system.

This more important problem noticed while testing was that the earlier assumed small friction force on the moving part of the system created by the sliders on the dyno was too large for the thrust to be applied by the propeller. The slide system consisted of two drawer guides that use ball bearings to create movement among the two parts of each slide. The friction created by the large weight of the components mounted to the free moving part of the dyno was very inconsistent during the calibration process. This inconsistency led the team to be unable to calibrate the new load cell. In order to measure a thrust force, the sliders must allow the free moving section to move, and this was not happening all the time. As force was applied in the thrust direction to the free moving part of the dyno, the sliders would react in different ways depending on the method that the load was applied. This is unacceptable as there is no way of knowing how the propeller applies its force, whether it is smooth and easier or harsh and rapidly. When 3 lbf were applied all at once, the sliders would allow the free moving section to move forward, but when the same total force was added 1 lb at a time, the sliders would not move. It took 5 lbf or sometimes 6 lbf of force to move the sliders when the force was applied 1 lbf at a time. It was determined that this was due to the ball bearings used in the sliders, and that coefficient of static friction in the cheap drawer sliders was just too large for the forces that are trying to measure.

Therefore a new method to create a free moving section of the dyno was researched heavily by the current team. It was determined that two linear rails was still the best method to use. A Igus DryLin N Low Profile Linear Guide System was purchased to take the place of the drawer guides. Two 10 in DryLin N-27-02 rails were purchased along with 2 NW-02-27 carriages and 2 NW-02-27-LLZ carriages. Two of the carriages purchased are designed so

they can float in the horizontal direction while two are fixed in the horizontal direction. This allows one side of the system to float horizontally which is necessary as it is extremely difficult to have two linear guides aligned perfectly. Figure 5.2.1.2-5 shows the one new DryLin N guide as well as both the drawer guides used before.

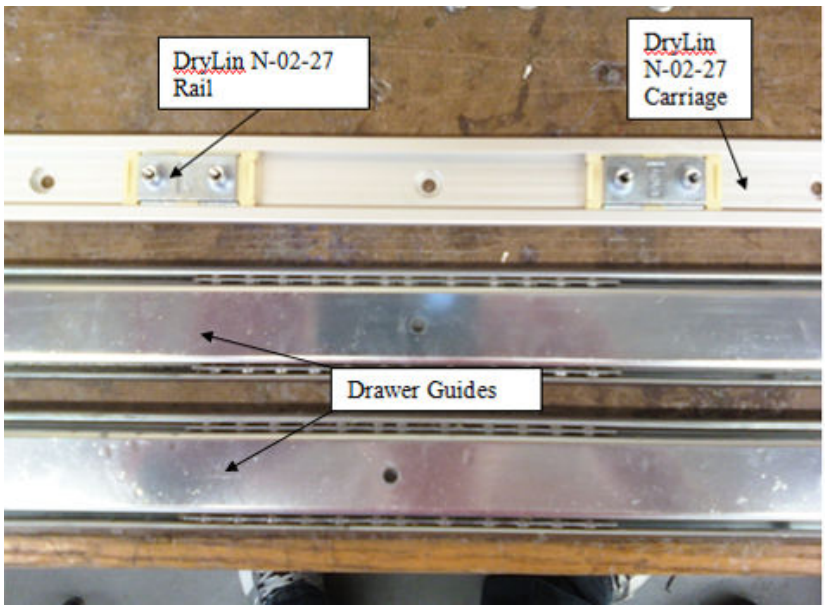

Figure 5.2.1.2-5: New DryLin N guide rail and old drawer guide rails

After several attempts to mount the new rail system to the dyno, this year's team's progress on fixing the dyno has come to a road block. The new system has proven to be very hard to install. In concept, the mounting should be simple, but the team has been unable to make it work. This is because the new rail system does not have enough play in it for our current set up. When mounting the metal carriages to the wooden dyno platform, no matter how much tweaking is done, the carriages will not line up enough to slide the rails over them. When trying to mount the wooden platform to the carriages already slide into the rails, there becomes no way to tighten the bolts connecting the two due to the rails being there. The solution to this would be to first mount metal strips to the bottom of the wooden platform with pre-aligned mounting holes where the carriages should mount to. This would ensure the carriages would be in the same vertical plane, and make it easier to align the carriages so they are in the same linear plane as well. This way the carriages would be mounted to the wooden

platform first, the rails slide on, and then the rails bottled to the wooden base of the dyno. Another option is the tap the carriage connection holes so a screw and be threaded into the carriages. This way the carriages can be loaded into the rails first, then rails and carriages would be mounted to the bottom side of the free moving section of the dyno. This will allow the carriages and the rails to be aligned in the horizontal and vertical directions. With this method, the only potential problem in the set up is the rails not being mounted to the dyno perfectly parallel. This should be relieved by two of the carriages being able to float in the horizontal direction. The mounting of the rails needs to be done before any static tests can be made. Currently the dyno has no rails mounted to it. Figure 5.2.1.2-6 below shows this and where the two rails will be mounted.

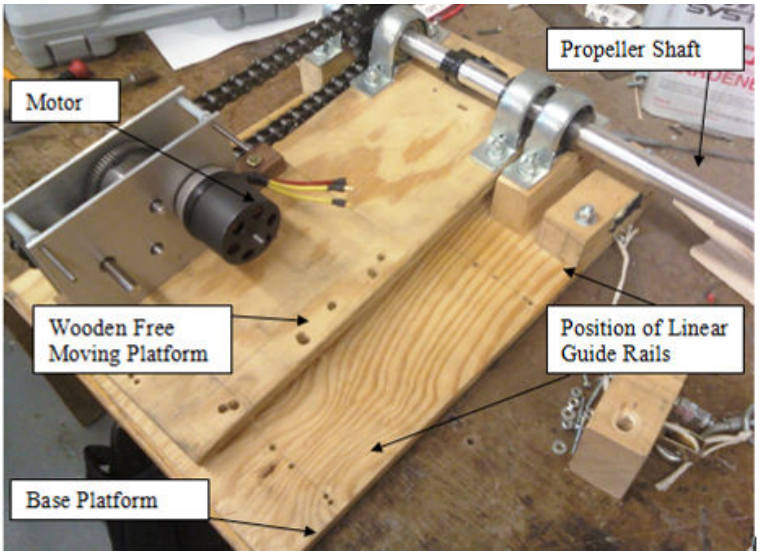

Figure 5.2.1.2-6: Dyno platform without rails

All that needs to be done in order to perform another calibration of the dyno system and then begin static and dynamic testing concerning the dyno is the new rail mounting and the re-amplifying of the load cell voltage. The previous team's method for getting the propeller in contact with a cruise speed free stream air velocity needs to be evaluated as well before dynamic testing can be done. This re-evaluation has been happening alongside the dyno rebuild.

The reason that there needs to be a new method for dynamic propeller testing is because the old method was very unsafe and introduced inertial loading back into the system. The test cart used in previous years is in very bad condition. It would most likely not last through another test run at 25.5 mph. It has been determined that the method of pulling the test cart with a long rope needs to be changed to take away the problem or inertial loading with the dyno. Many different concepts were discussed, and a new method has been selected. The current method will be to push the new drive train test cart from behind. The dyno can easily be mounted to the top portion of the new test cart. The new cart will definitely be able to with stand traveling that the cruise speed of the aircraft. The dyno will be controlled by LabView 8.2 as usual, but from the passenger seat of the push vehicle. This will make the dynamic testing much safer as well. It will be very easy to attach the test cart to the front of any truck to car with hooks under the front bumper and lock the steering of the front wheels of the test cart in the straight position. This will allow the people performing the test to be safe inside the push vehicle and should eliminate any unwanted acceleration of the test cart causing inertial forces on the free moving part of the dyno.

5.3 Wings

5.3.1 Wing Testing

Wing testing for the spring semester was originally planned to be a series of spar tests. The intention was to test a large number of various spar and strut configurations so that a wealth of technical data would be available for this team and following teams to use if wing design changes would be necessary. Early on, preparations were made with spar testing in mind.

While looking over previous reports [6], it was noticed that a wind tunnel test of a small wing section, shown below, indicated that the current spar location was insufficient.

The current spar location is at 35.6%, because computer analysis indicated that, theoretically, there should be no pitching moment at that location.

Figure 5.3.1-1: Earlier Wind Tunnel Test

Testing showed that that was not the case and that a strong, unexpected, pitch down moment was observed. This potentially jeopardized the entire wing design. Retrieving old XFOIL data from the FTP server showed the following relationship between angle of attack and pitching moment.

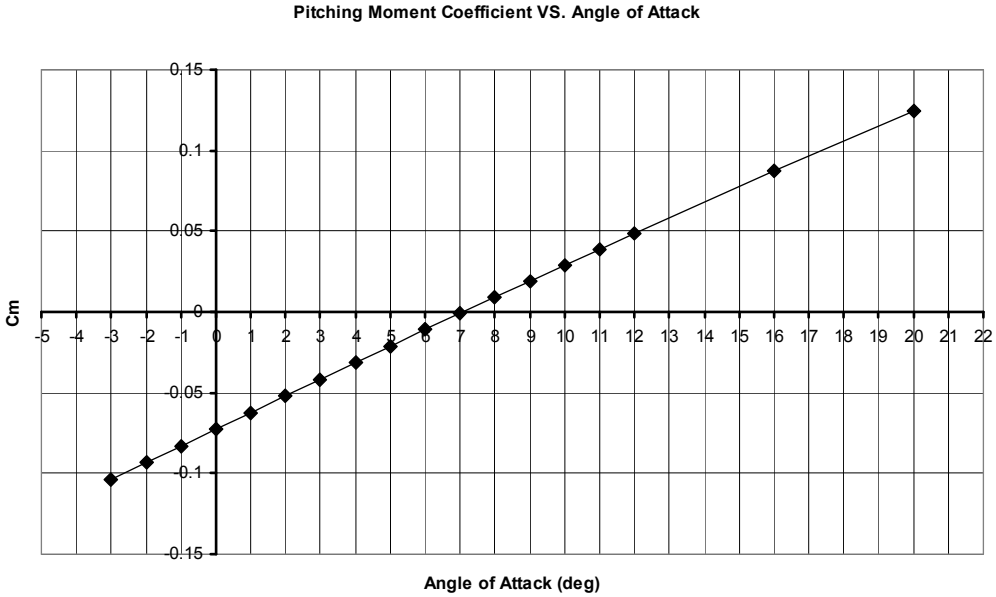

Figure 5.3.1-2: Pitching Moment Coefficient vs. Angle of Attack

The result of the previous team's experiment is not surprising given this data. Angle of attack is not statically stable. However, the lack of quantitative experimental data was an area that had to addressed.

It was decided that spar testing should be put on hold in favor of wing aerodynamic testing. The reason for this was that any redesign of the wing due to different aerodynamics would likely call for a redesign of the spar. However, the spar could, to some extent, be altered without affecting the airfoil.

The only facility that could easily be used to perform such a wind tunnel test is the Virginia Tech Stability Wind Tunnel. Discussions with the management of the wind tunnel revealed that our wing section would fit inside the test section if almost all of the protruding aluminum tube were cut off. Approval was given for a wind tunnel test contingent upon two conditions. One was preparing a mount to securely hold the wing section, so as to ensure that when testing came, the team would be prepared, and second was an accurate prediction of the forces and moments to be encountered by the wind tunnel sensors during our proposed testing regime, so as to ensure that the wind tunnel sensors and gauges would not be damaged during the test.

5.3.2 Wind Tunnel Mount

The team constructed the following wind tunnel mount out of wood, as seen in Figures 5.3.2-1 through 5.3.2-4. The team's mount is meant to attach to a calibration mount, which fits on the force and moment gauge used in the wind tunnel. The wing section slides onto the long wooden piece. It is estimated that friction will be sufficient to prevent the wing section from slipping during testing. The wing section will be mounted vertically in the test section and stretch from the wind tunnel sting to the top of the top section. Due to this, it was decided that induced drag would probably be negligible, and not need to be accounted for.

Figure 5.3.2-1: Wind Tunnel Mount, front view

Figure 5.3.2-2: Full View of Wind Tunnel Mount, front view

Figure 5.3.2-3: Wind Tunnel Mount with Wing Section

Figure 5.3.2-4: Wind Tunnel Mount with Wing Section, detail vie

Given the exact dimensions of the mount, and the expected forces and moments, it was simple to predict the forces and moments on the wind tunnel force and moment head. The only wind tunnel gauge restriction that the team has to keep in mind is the 41 N·m limit on rolling moment. The team originally wanted to test the wing section at various angles of attack from 5 to 40 miles per hour. As the following chart shows, that is not possible due to the expected loads, and the testing points highlighted in red, will have to be omitted. The remaining data points will still provide sufficient data to make the test worthwhile.

Table 5.3.2-1: Wind Tunnel Rolling Moment for Angle of Attack and Free Stream Velocity

Rolling Moment(N*m) U(mph) AOA(deg)	5	10	15	20	25	30	35	40
-2	0.24	0.95	2.14	3.80	5.93	8.54	11.63	15.19
0	0.37	1.49	3.34	5.94	9.29	13.37	18.20	23.77
2	0.51	2.02	4.55	8.08	12.63	18.18	24.75	32.32
4	0.64	2.55	5.74	10.21	15.95	22.97	31.26	40.83
6	0.77	3.08	6.93	12.32	19.25	27.72	37.73	49.28
8	0.90	3.60	8.11	14.41	22.52	32.43	44.14	57.66
10	1.03	4.12	9.27	16.49	25.76	37.09	50.49	65.94
12	1.16	4.63	10.42	18.53	28.95	41.69	56.75	74.12
16	1.41	5.63	12.67	22.53	35.20	50.68	68.99	90.10
20	1.65	6.59	14.84	26.37	41.21	59.34	80.77	105.50

As of the writing of this report, the team was still trying to get access to the wind tunnel to perform the test. If that cannot be obtained by this year's team, hopefully a testing day can be obtained for the team to follow us. If the team does get wind tunnel access, and whether or not the results can be included in the final report, any data will be saved and given to the next year's team as soon as possible with full explanation of its significance.

5.4 Tail

5.4.1 Tail Wing Test Plan

The load distribution on each wing was calculated using maximum lift coefficient of NACA0012 airfoil that was found from experimental data [10]. However the actual Reynolds

number is relatively low compared to the experimental data. The graphs of the load distribution and moment at the center are shown in Figure 5.4.1-2 and 5.4.1-3 for the horizontal and vertical respectively. To operate the test, this load distribution should be implemented on the spar. MATLAB programs were created to calculate the required weight and positioning of loads on the spar. The outputs of the program are shown in Table 5.4.1-1 and 5.4.1-2 for the horizontal and vertical respectively. By looking at this chart, the structure test can be easily performed.

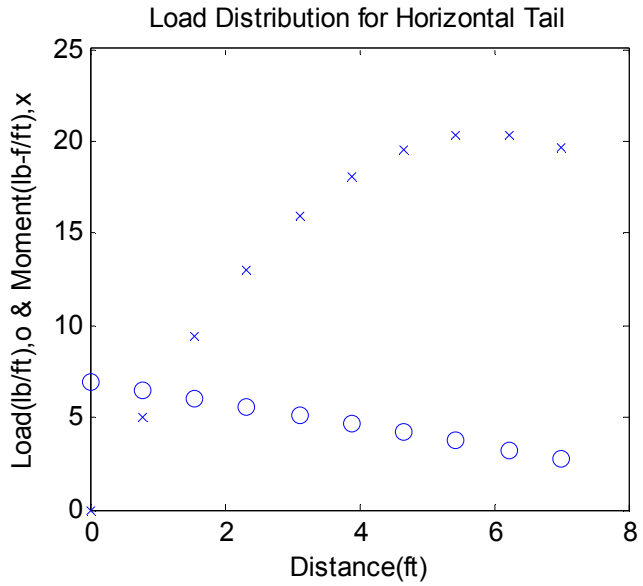

Figure 5.4.1-2: Graph of Load and Moment for Horizontal Tail (Half span)

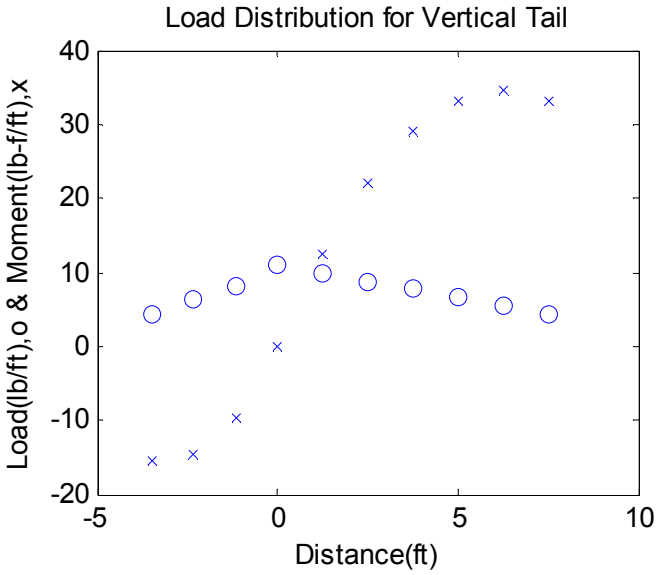

Figure 5.4.1-3: Graph of Load and Moment for Vertical Tail (Full span)

Table 5.4.1-1 Position and Load that needs to be applied for horizontal tail

Distance(in)	Weight(lb)
0	4.87
9.33	4.55
18.67	4.22
28	3.9
37.33	3.58
46.67	3.25
56	2.93
65.33	2.61
74.67	2.29
84	1.96

Table 5.4.1-2 Position and Load that needs to be applied for vertical tail

Distance(in)	Weight(lb)
0	11.82
15	10.64
30	9.46
45	8.28
60	7.1
75	5.92
90	4.74
Lower	Wing
14	9.52
28	7.34
42	5.16

5.4.2 Connector Test Plan

The maximum lift was calculated for both wings. To test the connectors, the maximum total lift must be applied to the connector. The Table 5.4.2-1 shows the load that should be applied for the connector test. If the structure fails, the thickness of the connector should be increased until the structure does not fail.

Table 5.4.2-1 Connector Test Plan

	Horizontal Tail	Vertical Tail
Weight(lb)	68.32	79.98

5.5 New 2009 Test Vehicle

5.5.1 Test Vehicle Configuration

The 2009 team created a new test vehicle made out of PVC for the purpose of testing the drivetrain system and the propeller. The test vehicle is rather larger and is stored in the Human Powered Aircraft Group trailer off of Plantation Road.

The vehicle is made out of 1.25 inch PVC piping. All the pieces have been cut and the vehicle has been assembled by hand. Two junior bicycles from Wal-Mart were cannibalized for their 16 inch wheels and various other parts. Currently, the steering linkage is connected, the front and rear wheels have been mounted, and the system is awaiting the drivetrain, driver's seat, and steering wheel. However, before any of these parts can be put on, tubes of steel reinforcement need to be run on the inside of the lower PVC beams that span the length and width of the test vehicle.

Finally, once the configuration is complete (drivetrain, steering, etc..) the vehicle should be cemented together using the PVC cement located in the Ware Lab. First, a thin lay of the PVC cleaning compound should be applied to a joint, then the PVC cement. After the cement has hardened, the alignment on the front wheels should be set to ensure a straight and smooth ride. A detailed outline of the components on the test vehicle can be seen in Figure 5.5.1-1 and 5.5.1-2.

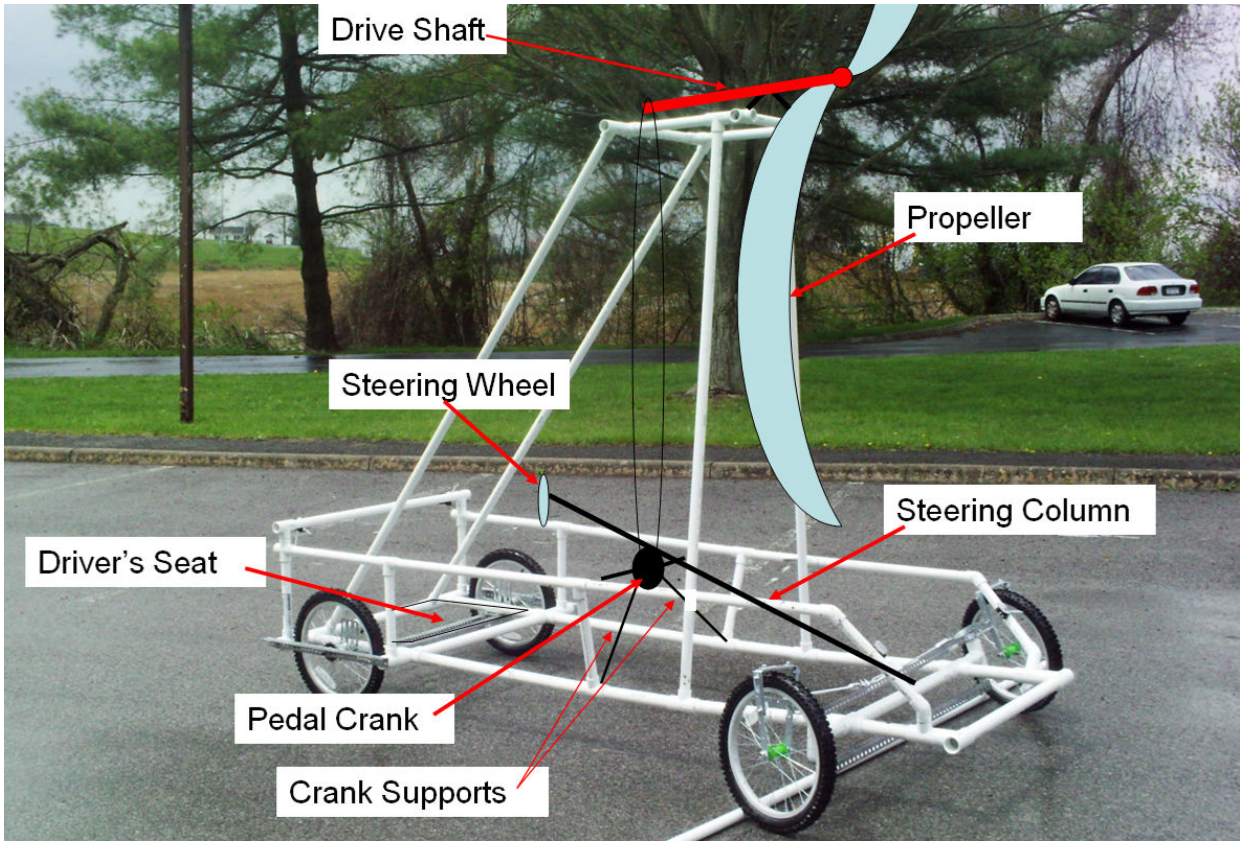

Figure5.5.1-1: Rendition of 2009 Test Vehicle Finished Product

Figure5.5.1-2: Back view of 2009 Test Vehicle

6. Project Status

6.1 Quarter-scale Model

Once the preliminary design of the aircraft was completed, the past teams constructed a quarter-scale model in order to validate the design. The construction and testing process was iterative, but ultimately successful. Testing of the quarter-scale model proved that a controlled turn performed by an aircraft of the current design is possible. This accomplishment is substantial because of its direct application to the achievement of the Kremer Price. The quarter scale model is currently disassembled and lacking major components required for flight. Its purpose has already been served and is not expected to provide further information.

6.2 Prototype

The majority of the components of the prototype are still in the final design stages. This process is iterative as changes made to a simple and small part, such as the exact location of the pilot seat, will have a profound impact on other parts of the plane. Currently the propeller, wings, and drivetrain are in the process of being tested, while the tail boom, tail wings, and cockpit are still being designed and or constructed.

7. Administration

7.1 Funding

The teams from the first two years operated exclusively on donations and sponsorships. This led to a method for recognizing sponsors, which is detailed in the 2006-2007 final report [5]. The third year's team received funding from the Ware Lab and has operated almost entirely from it. As a result, the team did not pursue sponsorship with the same rigor as the past teams. However the acknowledgement of past sponsors and the seeking of new ones will be a necessary occupation of future teams. Continued Ware Lab funding should be strongly pursued as well.

This year's team concentrated on obtaining funding from outside companies, in both monetary from and with materials. The only successful attempt to receive funds was contacting a family member at Lockheed Martin, who decided to donate $5000 to the HPA team after careful research into where the team is and how much more it needs to move forward. The team also received a donation from SolidWorks, a 3-D AutoCAD drawing company, which include ten SolidWorks AutoCAD programs to be used by both the HPA team and other senior design projects. More sponsors will be sought after, including cycling companies that may be interested in donating the parts necessary to get the propulsion and control surfaces to work. It will also be necessary to attempt to obtain funds and official school recognition from the SEC (Student Engineering Council) and SGA (Student Government Association) in the future to ensure the continuation of the project, and to generate more campus and national interest.

7.2 Budget

A definite budget for the construction of a full-scale aircraft has not yet been established. The second year's team proposed that the total cost of construction of a prototype aircraft to be well over eight thousand dollars [5]. Through the design and prototype construction phase of this project, a significant amount of this cost has already been accounted for in acquiring materials.

The third year's team received funds from the Ware Lab, which was a first for this project. The Ware Lab appropriated $2800 to the team for the year. The continuation of Ware Lab funding as well as the accruement of supplemental funding through donations or sponsorship will be essential for the continuation of this project. The second year's team left $375.72 in a separate foundation account for this project. This year's team inherited the previous year's funds, and added to the funds with a donation from Lockheed Martin. Table

7.1-1 lists the current financial balance of the team.

Table 7.1-1: Current financial balance

	State Account	Foundation Account
Balance	$768.94	$5,025.72

Most of the supplies for the project have been bought; it is just a matter of finalizing the design and determining the plan of construction. Once these factors have been taken care of it will just become a matter of determining what else needs to be bought and where else the money should be used

8. Summary

This is the fourth year of a multi-year design team with the goal of winning one of the current international Kremer Prizes. This report detailed the overall progress made this Spring 2009 semester. The three major sections of this report were the prototype design, construction, and testing aspects of the airplane.

The purpose of this report was to present a comprehensive description of the progress made this semester as well as to outline for next years team where to begin.

9. References

1. McIntyre, John. Human Powered Flight Group. March 2007. Royal Aeronautic Society. <http://www.raes.org.uk/cmspage.asp?cmsitemid=SG_Hum_Pow_Home>.

2. Kremer Human Powered Aircraft for Sport Rules and Regulations. May 2009 < http://www.raes.org.uk/cms/uploaded/files/SG_HPAG_sport.pdf>.

3. Spring 2005 HPA Iron Butterfly Final Report. <www.hpag.org.vt.edu>

4. Spring 2006 HPA Iron Butterfly Final Report. <www.hpag.org.vt.edu>

5. Spring 2007 HPA Iron Butterfly Final Report. <www.hpag.org.vt.edu>

6. Spring 2008 HPA Iron Butterfly Final Report. <www.hpag.org.vt.edu>

7. ANSYS, Inc. ANSYS 11. <http://www.ansys.com/>, 2009.

8. American Speedster. <http://www.americanspeedster.com/>, 2009

9. Matlab R2008a. < http://www.mathworks.com/>, 2009

10. Theory of Wing Sections by Ira Herbert Abbott, Albert Edward Von Doenhoff

10. Programs

a. ANSYS Cockpit test

This code will determine the structural analysis of the cockpit framework and output a diagram of the cockpit with different sections of the cockpit colored in a different color, where each color is a different range of the stresses.

```
!This text file was created by Scott Hutchinson with some help from Fred McMahon in the Spring Semester 2009

/title, COCKPIT ANALYSIS

/PREP7

!-----------------------------
!               GUI Filtering (Not known if needed)
!-----------------------------
!Structural is the only one set
KEYW,PR_SET,1
KEYW,PR_STRUC,1
KEYW,PR_THERM,0
KEYW,PR_FLUID,0
KEYW,PR_ELMAG,0
KEYW,MAGNOD,0
KEYW,MAGEDG,0
KEYW,MAGHFE,0
KEYW,MAGELC,0
KEYW,PR_MULTI,0
KEYW,PR_CFD,0
!-----------------------------
!               Creates the Seat coordinates
!-----------------------------
x11=44.75-6*cos(3.14159/6)
y11=1.299+6*sin(3.14159/6)
x12=x11
!-----------------------------
!               KEYPOINTS
!-----------------------------
!FORMAT: k,Keypoint Number,x,y,z
!
k,1,0,0,0
k,2,0,60,0
k,3,44,60,0
k,4,88.25,60,0
k,5,44,0,0
k,6,44,60,-10
k,7,44,60,10
k,8,44,0,-10
k,9,44,0,10
k,10,44.75,1.299,0
k,11,x11,y11,0
k,12,x12,0,0
k,13,45,0,0
!-----------------------------
!    Connecting Keypoints
!-----------------------------
!FORMAT: LSTR,Keypoint1,Keypoint2
!
LSTR,      1,            2
LSTR,      2,            3
LSTR,      3,            4
```

```
LSTR,     4,          10
LSTR,     10,         13
LSTR,     13,         5
LSTR,     5,          1
LSTR,     10,         11
LSTR,     11,         12
!*
!*        Connecting Z Keypoints
!*
LSTR,     3,          6
LSTR,     3,          7
LSTR,     5,          8
LSTR,     5,          9
LSTR,     6,          8
LSTR,     7,          9
!---------------------------
!         Local Element From Library
!---------------------------
!FORMAT: ET,Name,Element Type(BEAM4=3D Elastic Beam),
!
ET,1,BEAM4
!---------------------------
!         Element Length
!---------------------------
!FORMAT: ESIZE,Length,Default Number of Divisions
!*NOTE: If length is not input, it will rely on Default number of divisions
!*otherwise it is not used.
!
ESIZE,3,0
!---------------------------
!         Generating Nodes and Line Elements
!---------------------------
!FORMAT:LMESH,NL1,NL2
!*NOTE: If NL1 = ALL, NL2 is ignored
LMESH,ALL
!---------------------------
!         Forces
!---------------------------
!FORMAT:FK,Keypoint of force applied, Force Label(ie.FX),Value
!
FK,2,FX,-5.5
FK,4,MX,-86
FK,4,MY,-637,
FK,4,MZ,-822
FK,10,FY,-140
FK,11,FX,86
!---------------------------
!         Constraints
!---------------------------
!FORMAT:DK,Keypoints constraints are applied,Valid Degree of Freedom(ie.UX),DOF Value,
!
DK,1,ALL
DK,5,ALL
!---------------------------
!         Define Tube Properties
!---------------------------
!Tube
OD = 2.000                                  ! tube outer diameter
wall  = 0.032                               ! tube wall thickness
ID = OD-2*wall                              ! tube inner diameter
Areas = 3.14159/4*(OD**2-ID**2)             ! tube cross section area
Izzs = 3.14159/64*(OD**4-ID**4)             ! moment of inertia in zz
Iyys = Izzs                         ! moment of inertia in yy
!---------------------------
!         Material Properties
!---------------------------
! Material 1 - Aluminum 6061 Properties
Ex1 = 1e7                           ! young's modulus
v1 = 0.3                            ! poisson's ratio
! Material 2 - Carbon Fiber Properites
```

```
!Ex2 =1.8e7                                    ! young's modulus
!v2 =
!--------------------------
!           Defining Element Constants
!--------------------------
!FORMAT:R,Identification Number,AREA,IZZ,IYY,THICKZ,THICKY,THETA,ISTRN,IXX,SHEARZ,SHEARY,SPIN,ADDMASS
R,1,Areas, Izzs, Iyys
!
!FORMAT:MPTEMP,Starting Location in Table,Temperature Assigned to first location
!           MPDATA,Elastic Modulus,Element Number,Starting Location in Table,Value
!           MPDATA,Major Poissons Ratio,Element Number,Starting Location in Table,Value
MPTEMP,1,0
MPDATA,EX,1,1,Ex1
MPDATA,PRXY,1,1,v1
!--------------------------
!           Solution!
!--------------------------
/SOLU
SOLVE
!
/post1
!
!           Setting Up Element Table
!
ETABLE,SMAXI,NMISC,1
ETABLE,sMAXJ,NMISc,3
PLLS,SMAXI,SMAXJ,1,0
```

b. Matlab Seat/Pedal Positioning

This code takes the properties of the cockpit, specifies where the pedals are, and gives a range of values for the seat location, leg distance and seat angle.

```
for w=0:0.5:16
   x1=84-(15+60*tan(pi/6));  % This is the x distance from the front of the cockpit to the support bars
   x2=x1-(18-w);  % This is the x distance from the pedals to the support bars
   xs=7.490323*12-w;  % This is the point on the cockpit where the shoulders are at the thinnest possible point
   x4m=xs-x1;  % This is the maximum value of x4
   fprintf('Distance the airfoil start to the front of the cockpit (in inches)  \n')
   fprintf('-------------------------------------------------------------------\n')
   fprintf('                        [%2.1f]                    \n',w)
   fprintf('x3        y1        y2        z        theta        xshoulder   \n')
   fprintf('-------------------------------------------------------------------------------\n')
   for x3=0.5:0.5:40
      y1=x3*tan(pi/3);  % This is the height of the seat from the bottom of the cockpit
      y2=24-y1;  % This is the y distance from the pedals to the seat
      z=sqrt(y2^2+(x2+x3)^2);  % This is the straight line (hypotenuse) distance from the seat to the pedals
      theta=asind(y2/z);
      if theta<29
         break
      end
      a=sqrt(x3^2+y1^2);  % This is the hypotenuse distance along the bar from the bottom of the cockpit to the seat
      b=20+a; % This is the hypotenuse distance along the bar from the bottom of the cockpit to the pilots shoulders
      x4=b*sin(pi/6);  % This is the x distance from the seat to the pilots shoulders
      if x4>x4m
         break
      end
      xshoulder=x4+x1;  % This is the x distance from the front of the cockpit to the pilots shoulders
      fprintf('%2.1f     %2.4f     %2.4f     %2.4f     %2.4f     %2.4f\n',x3,y1,y2,z,theta,xshoulder)
   end
end
```

c. Matlab Ribs dimensions for Horizontal tail

```
nRib = input('\nEnter number of Ribs for Horizontal Tail(odd): ');

A = 28; %ft^2
b = 14; %ft
TR = 2.5;
Naca = 12; %NACA 00XX

cMin = A*2/(b*(1+TR));
cMax = cMin*TR;

inc = b/(nRib-1);

iHalf = (nRib-1)/2+1;

bTest = 0;
ATest = 0;
c(1) = cMin;
for i =1:iHalf-1
    c(i+1) = c(i)+(cMax-cMin)/(iHalf-1);
    bTest = bTest+inc;
    ATest = ATest+c(i)*inc;
end

c(iHalf) = cMax;

for i =iHalf:nRib-1
    c(i+1) = c(i)-(cMax-cMin)/(iHalf-1);
    bTest = bTest+inc;
    ATest = ATest+c(i)*inc;
end

c(nRib) = cMin;

fprintf('\nRib#    ')
fprintf('Chord Length(inch)    ')
fprintf('Spar position(inch)    ')
fprintf('Maximum Thickness(inch)     ')
fprintf('Rib thickness(inch)\n')

for i =1:nRib
    fprintf('%3.0f',i)
    fprintf('%17.5f',c(i)*12) %inch
    fprintf('%22.5f',c(i)*0.3*12) %inch
    fprintf('%24.5f',c(i)*Naca/100*12) %inch
    fprintf('%24.5f\n',c(i)*Naca/100*12*0.1) %inch
end

fprintf('\nSpace between Ribs is: %.5f ft',inc)
fprintf('\nDiameter of Spar is: %.5f inch\n',c(1)*Naca/100*0.90*12)
```

d. Matlab Ribs dimensions for Vertical tail

```
nRibUp = input('\nEnter number of Ribs above boom:  ');
nRibBelow = input('Enter number of Ribs below boom:  ');

nRib = nRibUp + nRibBelow +1;

AR = 3.5;
b = 11;
bBelow = 3.5;
TR = 2.5;
Naca = 12; %NACA 00XX

cAve = b/AR;
```

```
bUp = b - bBelow;

cMin = cAve*2/(1+TR);
cMax = cMin*TR;

incUp = (b-bBelow)/(nRibUp);

iHalf = nRibUp+1;

bTest = 0;
ATest = 0;
c(1) = cMin;
for i =1:iHalf-1
    c(i+1) = c(i)+(cMax-cMin)/(iHalf-1);
    bTest = bTest+incUp;
    ATest = ATest+c(i)*incUp;
end

c(iHalf) = cMax;
incBelow = bBelow/((nRib-nRibUp)-1);

for i =iHalf:nRib-1
    c(i+1) = c(i)-(cMax-cMin)/(nRib-iHalf);
    bTest = bTest+incBelow;
    ATest = ATest+c(i)*incBelow;
end

c(nRib) = cMin;

fprintf('\nRib#  ')
fprintf('Chord Length(inch)  ')
fprintf('Spar position(inch)    ')
fprintf('Maximum Thickness(inch)     ')
fprintf('Rib thickness(inch)\n')

for i =1:nRib
    fprintf('%3.0f',i)
    fprintf('%17.5f',c(i)*12) %inch
    fprintf('%22.5f',c(i)*0.3*12) %inch
    fprintf('%24.5f',c(i)*Naca/100*12) %inch
    fprintf('%24.5f\n',c(i)*Naca/100*12*0.1) %inch
end

fprintf('\nSpace between Ribs above boom: %f ft\n',incUp)
fprintf('Space between Ribs below boom: %f ft',incBelow)
fprintf('\nDiameter of Spar is: %f in\n',c(1)*Naca/100*0.90*12)
fprintf('NACA 00%.0f airfoil\n',Naca)
```

e. Matlab Load calculation for Structure test for Horizontal tail

```
Clmax = 1.6;
v = 24.5; %mph
v = v*5280/3600; %f/s
ro = 0.0023769; %slug/ft^3

b = 7; %ft
h = 10; %number of calculation

dx = b/h; %delta x, ft
x = linspace(0,b,h);
c = linspace(34/12,13.7/12,h);
L = Clmax*(1/2)*(v^2)*ro.*c;
M = L.*x;

plot(x,L,'o')
xlabel('Distance(ft)');
ylabel('Load(lb/ft),o & Moment(lb-f/ft),x');
```

```
title('Load Distribution for Horizontal Tail')
hold on
plot(x,M,'x')

sumL = 2*sum(L)*dx;

fprintf('\n-- Table of Load Distribution for Horizontal Tail  --')
fprintf('\n Distance(in)  Weight(lb)\n')
for i = 1:h
    fprintf('%10.2f %10.2f\n',x(i)*12,L(i)*dx)
end
fprintf('Total weight is: %.2f lb\n',sumL)
```

f. Matlab Load calculation for Structure test for Vertical tail

```
Clmax = 1.6;
v = 24.5; %mph
v = v*5280/3600; %f/s
ro = 0.0023769; %slug/ft^3

bu = 7.5; %ft
bb = 3.5;
hu = 7; %number of calculation
hb = 3;

dxu = bu/hu; %delta x, ft
dxb = bb/hb; %delta x, ft

xu = linspace(0,bu,hu);
xb = linspace(-dxb,-bb,hb);
cu = linspace(53.9/12,21.6/12,hu);
cb = linspace(53.9/12-dxb,21.6/12,hb);
Lu = Clmax*(1/2)*(v^2)*ro.*cu;
Lb= Clmax*(1/2)*(v^2)*ro.*cb;
Mu = Lu.*xu;
Mb = Lb.*xb;

plot(xu,Lu,'o')
hold on
plot(xb,Lb,'o')
plot(xu,Mu,'x')
plot(xb,Mb,'x')
xlabel('Distance(ft)');
ylabel('Load(lb/ft),o & Moment(lb-f/ft),x');
title('Load Distribution for Vertical Tail')

sumL = sum(Lu)*dxu + sum(Lb)*dxb;

fprintf('\n-- Table of Load Distribution for Vertical Tail  --')
fprintf('\n--- Upper Wing ---')
fprintf('\n Distance(in)  Weight(lb)\n')
for i = 1:hu
    fprintf('%10.2f %10.2f\n',xu(i)*12,Lu(i)*dxu)
end
fprintf('--- Lower Wing ---\n')
for i = 1:hb
    fprintf('%10.2f %10.2f\n',-xb(i)*12,Lb(i)*dxb)
end
fprintf('Total weight is: %.2f lb\n',sumL)
```

g. Determining CG Location

```
%%%%%%%%%%%%%%%%%%%%%%%%%%%%%%%%%%%%%%%%%%%%%%%%%%%%%%%%%%%%%%%%%%%%%%%%%%%%
%           DETERMINING CG_tot LOCATION (CG_totSolving.m)                %
%%%%%%%%%%%%%%%%%%%%%%%%%%%%%%%%%%%%%%%%%%%%%%%%%%%%%%%%%%%%%%%%%%%%%%%%%%%%
%
% This program uses the volumes of cylinders and densities of
% aluminum and carbon fiber to determine where the CG_tot
% of the aircraft should be, and what the error is without the pilot.
% Currently plotted: Wing Spars and Struts, Tail Boom, Horizontal
% Tail, Vertical Tail, and Propellor. The Propellor is used to
% determine the CG location but needs to be added to the graphs.
% The best location for the pilot will eventually be determined
% by this program. Notes have been made for where this should occur
% in the program.

%% Material Properties
%%Aluminum - Al 6061-T6%%
Al_mod = 1.00E+07; %Aluminum Modulus of Elasticity, psi
Al_pos = 0.3; %Aluminum Poisson's Ratio
Al_rho = 0.0975; %Aluminum Density, lb/in^3

%%Carbon Fiber%%
C_mod = 1.48E+07; %Carbon Fiber Modulus of Elasticity, psi
C_pos = 0.3; %Carbon Fiber Poisson's Ratio
C_rho = 0.055; %Carbon Fiber Density, lb/in^3
%Carbon fiber info may need to be corrected, check a materials book.

%% WING INNER SPAR DIMENSIONS %%
%See hpa_s2_final_rev5.pdf (2006 - 2007 Final Report), pg 45
Spars_Inner_Length = 48*12; %TOTAL Inner Spars Length in inches
Spar_I_Length = Spars_Inner_Length/4; %Inner Spars Length in inches
Spar_I_OD     = 2;  %Inner Spar Outer Diameter, inches
Spar_I_ID     = 1.944; %Inner Spar Inner Diameter, inches

%% WING OUTER SPAR DIMENSIONS %%
%See hpa_s2_final_rev5.pdf (2006 - 2007 Final Report), pg 45
Spars_Outer_Length = 72*12; %TOTAL Outer Spars Length in inches
Spar_O_Length = Spars_Outer_Length/4; %Outer Spars Length in inches
Spar_O_OD     = 1.75;  %Outer Spar Outer Diameter inches
Spar_O_ID     = 1.718; %Outer Spar Inner Diameter, inches

%% WING INNER STRUT DIMENSIONS - Also known as Strut 1 %%
%See hpa_s2_final_rev5.pdf (2006 - 2007 Final Report), pg 45
Struts_Inner_Length = 10*12;
Strut_I_Height = Struts_Inner_Length/2; %Inner Strut Height in inches
Strut_I_OD     = 1.5;  %Inner Strut Outer Diameter, inches
Strut_I_ID     = 1.388; %Inner Strut Inner Diameter, inches

%% WING OUTER STRUT DIMENSIONS - Also known as Strut 2 %%
%See hpa_s2_final_rev5.pdf (2006 - 2007 Final Report), pg 45
Struts_Outer_Length = 10*12;
Strut_O_Height = Struts_Outer_Length/2; %Outer Strut Length in inches
Strut_O_OD     = 1;  %Inner Strut Outer Diameter, inches
Strut_O_ID     = 0.960; %Inner Strut Inner Diameter, inches
```

```
%% TAIL BOOM DIMENSIONS %%
TailBoom_Length = 20.7*12; %Tail Boom Length, inches, DUMMY VALUE
TailBoom_ID = 4; % Tail Boom Inner Diameter, inches
TailBoom_OD = 4.08; %Inches, DUMMY VALUE
%NEXT VAL IS A DUMMY VALUE?
TailBoom_InFront = 4*12; %How much of the tail boom is before wing spars

%% HORIZONTAL TAIL DIMENSIONS %%
TailHz_Spar_OD = 1.481143; %Inches, POSSIBLY DUMMY VALUE?
TailHz_Spar_ID = 1.42; %Inches, DUMMY VALUE
TailHz_Span = 14*12; %Inches
TailHz_Location = -24; %Inches, from TailBoom End, DUMMY VALUE

%% VERTICAL TAIL (Spar) DIMENSIONS %%
TailVt_Spar_OD = 2.32751; %Inches, DUMMY VALUE?
TailVt_Spar_ID = 2.262751; %Inches, DUMMY VALUE?
TailVt_Span = 11*12; %Inches
Tail_Vt_SpanBelowBoom = 3.5*12; %Inches
TailVt_Location = 6; %Inches, From TailBoom End, DUMMY VALUE
%Estimated values from 2008-2009 fall report...

%% FUSELAGE/COCKPIT DIMENSIONS/LOCATIONS %%
Cockpit_OD = 2.000;
Cockpit_WallThickness = 0.032;
Cockpit_ID = Cockpit_OD - 2*Cockpit_WallThickness; % = 1.9360

%% PROPELLOR DIMENSIONS/LOCATIONS %%
Propellor_wt = 2.00; %ESTIMATE
Propellor_loc = 0; %FROM FRONT OF TAIL BOOM

%% DRIVE TRAIN WEIGHTS
%NO CURRENT LOCATION IS SET!

%% PILOT WEIGHT/LOCATIONS
Pilot_wt = 148; %lbs, current estimate.

%% TARGET CG LOCATION
Target_x = 0;   Target_y = 0;    Target_z = 0;
%Will need to be confirmed by 2009-2010 Team.

%% SET THE MATERIAL PROPERTIES OF THE SPARS & STRUTS, lb/in^3 %%
%Currently, everything is made out of aluminum....
Spar_I_rho    = C_rho;   Spar_O_rho    = C_rho;
Strut_I_rho   = C_rho;   Strut_O_rho   = C_rho;
TailBoom_rho  = C_rho;   Cockpit_rho   = C_rho;
TailHz_Spar_rho = C_rho;  TailVt_Spar_rho = C_rho; %Both Subject to change


%% GET THE VOLUMES OF EACH, in^3 %%
%Using the volume equation for hollow cylinder.
Spar_I_vol = pi*(Spar_I_OD^2/4-Spar_I_ID^2/4)*Spar_I_Length;
Spar_O_vol = pi*(Spar_O_OD^2/4-Spar_O_ID^2/4)*Spar_O_Length;
Strut_I_vol = pi*(Strut_I_OD^2/4-Strut_I_ID^2/4)*Strut_I_Height;
Strut_O_vol = pi*(Strut_O_OD^2/4-Strut_O_ID^2/4)*Strut_O_Height;
TailBoom_vol = pi*(TailBoom_OD^2/4-TailBoom_ID^2/4)*TailBoom_Length;
```

```
TailHz_Spar_vol = pi*(TailHz_Spar_OD^2/4-TailHz_Spar_ID^2/4) ...
    *TailHz_Span; %DUMMY VALUE
TailVt_Spar_vol = pi*(TailVt_Spar_OD^2/4-TailVt_Spar_ID^2/4) ...
    *TailVt_Span; %DUMMY VALUE

%% GET THE WEIGHT OF EACH, lbs %%
%Multiplying volume by the density
Spar_I_wt = Spar_I_vol*Spar_I_rho;     % = 4.8709 lbs
Spar_O_wt = Spar_O_vol*Spar_O_rho;     % = 3.6712 lbs
Strut_I_wt = Strut_I_vol*Strut_I_rho; % = 2.9723 lbs
Strut_O_wt = Strut_O_vol*Strut_O_rho; % = 0.7204 lbs
TailBoom_wt = TailBoom_vol*TailBoom_rho; % = 12.2955 lbs
TailHz_Spar_wt = TailHz_Spar_vol*TailHz_Spar_rho; %DUMMY VALUE
TailVt_Spar_wt = TailVt_Spar_vol*TailVt_Spar_rho; %DUMMY VALUE

%% GET THE WEIGHT OF EACH IF HAVE TWO WINGS, lbs %%
%OF ONE SIDE!
Spar_I_wt_tot = Spar_I_vol*Spar_I_rho*2;      % =  lbs
Spar_O_wt_tot = Spar_O_vol*Spar_O_rho*2;      % =  lbs
Strut_I_wt_tot = Strut_I_vol*Strut_I_rho;     % =  lbs
Strut_O_wt_tot = Strut_O_vol*Strut_O_rho;     % =  lbs

Spar_tot = Spar_I_wt_tot + Spar_O_wt_tot;     % = 4.8186 lbs
%Spar_tot*2 % = 9.6373 lbs (Both sets of wings)
Strut_tot = Strut_I_wt_tot + Strut_O_wt_tot; % = 1.0415 lbs
%Strut_tot*2 % = 2.0831 lbs (Both sets of wings)
Spar_Strut_Total_Wt = Spar_tot + Strut_tot; % = 5.8602 lbs

Spar_Strut_Both_Sides_Wt = Spar_Strut_Total_Wt*2; % = 11.7203 lbs
Tail_Wt = TailBoom_wt + TailHz_Spar_wt + TailVt_Spar_wt;
% TotalWeight = Spar_Strut_Both_Sides_Wt + TailBoom_wt;
TotalWeight2 = Spar_Strut_Both_Sides_Wt + Tail_Wt + Propellor_wt;
TotalWeightPilot = TotalWeight2 + Pilot_wt; %Weight with pilot


%% NOW TO FIND THE CG OF EACH! %%

%On the horizontal axis, from left, from bottom reference point
%on each component--
Spar_I_cg_hz = Spar_I_Length/2;
Spar_O_cg_hz = Spar_O_Length/2;
Strut_I_cg_hz = Strut_I_OD/2;
Strut_O_cg_hz = Strut_O_OD/2;
TailBoom_cg_hz = TailBoom_OD/2;
TailHzSpar_cg_hz = TailHz_Span/2; %DUMMY VALUE
TailVtSpar_cg_hz = TailVt_Spar_OD/2; %DUMMY VALUE

%On the vertical axis, from bottom reference point
Spar_I_cg_vt = Spar_I_OD/2;
Spar_O_cg_vt = Spar_O_OD/2;
Strut_I_cg_vt = Strut_I_Height/2;
Strut_O_cg_vt = Strut_O_Height/2;
TailBoom_cg_vt = TailBoom_OD/2;
TailHzSpar_cg_vt = TailHz_Spar_OD/2; %DUMMY VALUE
TailVtSpar_cg_vt = TailVt_Span/2; %DUMMY VALUE
```

```
%Now convert to middle of wings!
%% GET HORIZONTAL CG COMPONENTS
Spar_I_cg_hzc = Spar_I_cg_hz;
Spar_O_cg_hzc = Spar_I_Length + Spar_O_cg_hz;
Strut_I_cg_hzc = Spar_I_Length;
Strut_O_cg_hzc = Spar_I_Length+Spar_O_Length-Spar_O_OD/2;
TailBoom_hzc   = 0;
TailHzSpar_cg_hzc = 0; %DUMMY VALUE, BUT CORRECT
TailVtSpar_cg_hzc = 0; %DUMMY VALUE, BUT CORRECT
Propellor_cg_hzc = 0; %DUMMY VALUE, BUT CORRECT


Sum_Hz_Right = (2*Spar_I_cg_hzc*Spar_I_wt) + (2*Spar_O_cg_hzc*Spar_O_wt)...
    + (Strut_I_cg_hzc*Strut_I_wt) + (Strut_O_cg_hzc*Strut_O_wt);
Sum_Hz_Left = -Sum_Hz_Right;
Sum_Hz_TailSpars = (TailBoom_hzc*TailBoom_wt) + (TailHzSpar_cg_hzc* ...
    TailHz_Spar_wt) + (TailVtSpar_cg_hzc*TailVt_Spar_wt); %DUMMY VALUE
Sum_Hz2 = (Sum_Hz_Right + Sum_Hz_Left + Sum_Hz_TailSpars + ...
    Propellor_wt*Propellor_cg_hzc)/TotalWeight2;

%% GET VERTICAL CG COMPONENTS
Spar_I_cg_vtc = Strut_I_cg_vt+Spar_I_OD/2;
Spar_O_cg_vtc = Strut_O_cg_vt+Spar_O_OD/2;
Strut_I_cg_vtc = 0;
Strut_O_cg_vtc = 0;
TailBoom_vtc  = Strut_I_Height/2-TailBoom_cg_vt;
TailHzSpar_cg_vtc = Strut_I_Height/2-TailBoom_OD- ...
    TailHzSpar_cg_vt; %DUMMY VALUE
TailVtSpar_cg_vtc = TailBoom_vtc-Tail_Vt_SpanBelowBoom + ...
    TailVtSpar_cg_vt; %DUMMY VALUE
Propellor_cg_vtc = TailBoom_vtc; %SINCE CONNECTED TO TAIL BOOM, DUMMY VAL

Sum_Vt_Right = Spar_I_cg_vtc*Spar_I_wt - Spar_I_cg_vtc*Spar_I_wt + ...
    Spar_O_cg_vtc*Spar_O_wt - Spar_O_cg_vtc*Spar_O_wt + ...
    Strut_I_cg_vtc*Strut_I_wt + Strut_O_cg_vtc*Strut_O_wt;
Sum_Vt_Left = -Sum_Vt_Right;
Sum_Vt_TailSpars = (TailBoom_vtc*TailBoom_wt) + (TailHzSpar_cg_vtc* ...
    TailHz_Spar_wt) + (TailVtSpar_cg_vtc*TailVt_Spar_wt); %DUMMY VALUE
% Sum_Vt = (Sum_Vt_Right + Sum_Vt_Left + TailBoom_vtc*TailBoom_wt)/ ...
%           TotalWeight;
Sum_Vt2 = (Sum_Vt_Right + Sum_Vt_Left + Sum_Vt_TailSpars + ...
    Propellor_cg_vtc*Propellor_wt)/TotalWeight2; %DUMMY VALUE

%% GET THIRD CG COMPONENTS
Spar_I_cg_zc = 0;
Spar_O_cg_zc = 0;
Strut_I_cg_zc = 0;
Strut_O_cg_zc = 0;
TailBoom_cg_zc = TailBoom_Length/2-TailBoom_InFront;
TailHzSpar_cg_zc = TailBoom_cg_zc + TailBoom_Length/2 + TailHz_Location;
TailVtSpar_cg_zc = TailBoom_cg_zc + TailBoom_Length/2 + TailVt_Location;

%PROPELLOR CONNECTED TO FRONT OF TAILBOOM, DUMMY VALUE BUT CORRECT
Propellor_cg_zc = TailBoom_cg_zc - TailBoom_Length/2 + Propellor_loc;
```

```
Tail_Sum_z = (TailBoom_cg_zc*TailBoom_wt) + (TailHzSpar_cg_zc* ...
    TailHz_Spar_wt) + (TailVtSpar_cg_zc*TailVt_Spar_wt); %DUMMY VALUE

Sum_z_wing = 4*Spar_I_cg_zc*Spar_I_wt + 4*Spar_O_cg_zc*Spar_O_wt ...
    + 2*Strut_I_cg_zc*Strut_I_wt + 2*Strut_O_cg_zc*Strut_O_wt;

Sum_z = (Tail_Sum_z+Sum_z_wing + Propellor_cg_vtc*Propellor_cg_zc ...
    )/TotalWeight2;

%% DETERMINE HOW FAR OFF CURRENT CG_tot IS FROM TARGET CG_tot

Error_x = Target_x - Sum_Hz2
Error_y = Target_y - Sum_Vt2
Error_z = Target_z - Sum_z

%% DETERMINE BEST LOCATION FOR PILOT
%To be done in the future.

%% FRONT VIEW: Draw the 2D Geometry! %%
%Center of wings will be at origin!
figure;

%% Horizontal Tail Spar
%Get the values needed for plotting
HzTS_x1 = -(TailHzSpar_cg_hzc + TailHz_Span/2);
HzTS_x2 = -HzTS_x1; %POSITIVE NUMBER
HzTS_y1 = TailHzSpar_cg_vtc + TailHz_Spar_OD/2;
HzTS_y2 = TailHzSpar_cg_vtc - TailHz_Spar_OD/2;

%Points to be used in the "box" shape
HzTailSpar_x_vals = [HzTS_x1 HzTS_x2 HzTS_x2 HzTS_x1 HzTS_x1];
HzTailSpar_y_vals = [HzTS_y1 HzTS_y1 HzTS_y2 HzTS_y2 HzTS_y1];

%Plot the horizontal tail
plot(HzTailSpar_x_vals,HzTailSpar_y_vals)
hold on

%% Plot everything in order necessary for legend
plot(Spar_I_cg_hzc,Spar_I_cg_vtc,'+k')
plot(Target_x,Target_y,'+g')
plot(Sum_Hz2,Sum_Vt2,'+r');
legend('Component Geometry', 'Component CG','CG Target', 'Empty Weight CG')

%% Vertical Tail Spar
%Get the values needed for plotting
VtTS_x1 = -(TailVtSpar_cg_hzc + TailVt_Spar_OD/2);
VtTS_x2 = -VtTS_x1; %POSITIVE VALUE
VtTS_y1 = TailVtSpar_cg_vtc + TailVt_Span/2;
VtTS_y2 = TailVtSpar_cg_vtc - TailVt_Span/2;

%Points to be used in the "box" shape
VtTailSpar_x_vals = [VtTS_x1 VtTS_x2  VtTS_x2   VtTS_x1  VtTS_x1];
VtTailSpar_y_vals = [VtTS_y1 VtTS_y1 VtTS_y2  VtTS_y2  VtTS_y1];
```

```
%Plot the horizontal tail
plot(VtTailSpar_x_vals,VtTailSpar_y_vals)

%% Tail Boom
%Get the center location and the circle's radius
TailBoom_x = TailBoom_hzc;
Tailboom_y = TailBoom_vtc;
TailBoom_r = TailBoom_OD/2;
%circle([TailBoom_hzc,TailBoom_vtc],TailBoom_r,100)
%FOR NOW, GOING TO MAKE A BOX!
TailB_x1 = TailBoom_x - TailBoom_r;
TailB_x2 = TailBoom_x + TailBoom_r;
TailB_y1 = TailBoom_vtc-TailBoom_OD/2;
TailB_y2 = TailBoom_vtc+TailBoom_OD/2;

TailB_x_vals = [TailB_x1 TailB_x2 TailB_x2 TailB_x1 TailB_x1];
TailB_y_vals = [TailB_y1 TailB_y1 TailB_y2 TailB_y2 TailB_y1];

plot(TailB_x_vals,TailB_y_vals)

%% Wing: Inner Spars
%Get the values needed for plotting
Spar_I_x1 = 0;
Spar_I_x2 = Spar_I_Length;
Spar_I_y1 = Strut_I_Height/2 + Spar_I_OD;
Spar_I_y2 = Strut_I_Height/2;

%Points to be used in the "box" shape
Spar_I_x_vals = [Spar_I_x1 Spar_I_x2 Spar_I_x2 Spar_I_x1 Spar_I_x1];
Spar_I_y_vals = [Spar_I_y1 Spar_I_y1 Spar_I_y2 Spar_I_y2 Spar_I_y1];

%Plot all four inner spars.
plot(Spar_I_x_vals, Spar_I_y_vals) %Plot right Upper IS
plot(Spar_I_x_vals, -Spar_I_y_vals) %Plot right Lower IS
plot(-Spar_I_x_vals, Spar_I_y_vals) %Plot left  Upper IS
plot(-Spar_I_x_vals, -Spar_I_y_vals) %Plot left  Lower IS

%% Wing: Outer Spars
%Get the values needed for plotting
Spar_O_x1 = Spar_I_Length;
Spar_O_x2 = Spar_O_x1 + Spar_O_Length;
Shift = (Spar_I_OD-Spar_O_OD)/2;
Spar_O_y1 = Strut_I_Height/2 + Shift + Spar_O_OD;
Spar_O_y2 = Strut_I_Height/2 + Shift;

%Points to be used in the "box" shape
Spar_O_x_vals = [Spar_O_x1 Spar_O_x2 Spar_O_x2 Spar_O_x1 Spar_O_x1];
Spar_O_y_vals = [Spar_O_y1 Spar_O_y1 Spar_O_y2 Spar_O_y2 Spar_O_y1];

%Plot all four outer spars.
plot(Spar_O_x_vals, Spar_O_y_vals)   %Plot right Upper OS
plot(Spar_O_x_vals, -Spar_O_y_vals)  %Plot right Lower OS
plot(-Spar_O_x_vals, Spar_O_y_vals)  %Plot left  Upper OS
plot(-Spar_O_x_vals, -Spar_O_y_vals) %Plot left Lower OS
```

```
%% Wing: Inner Struts
%Get the values needed for plotting
Strut_I_x1 = Spar_I_Length-Strut_I_OD/2; %Left Val
Strut_I_x2 = Spar_I_Length+Strut_I_OD/2; %Right Val
Strut_I_y1 = Strut_I_Height/2; %Higher Val
Strut_I_y2 = -Strut_I_Height/2; %Lower Val

%Points to be used in the "box" shape
Strut_I_x_vals = [Strut_I_x1 Strut_I_x2 Strut_I_x2 Strut_I_x1 Strut_I_x1];
Strut_I_y_vals = [Strut_I_y1 Strut_I_y1 Strut_I_y2 Strut_I_y2 Strut_I_y1];

%Plot both inner struts.
plot( Strut_I_x_vals,  Strut_I_y_vals) %Plot right IS
plot( -Strut_I_x_vals, Strut_I_y_vals) %Plot left IS

%% Wing: Outer Struts
%Get the values needed for plotting
Strut_O_x1 = Spar_I_Length+Spar_O_Length-Strut_O_OD; %Left Val
Strut_O_x2 = Spar_I_Length+Spar_O_Length; %Right Val
Strut_O_y1 = Strut_O_Height/2; %Higher Val
Strut_O_y2 = -Strut_O_Height/2; %Lower Val

%Points to be used in the "box" shape
Strut_O_x_vals = [Strut_O_x1 Strut_O_x2 Strut_O_x2 Strut_O_x1 Strut_O_x1];
Strut_O_y_vals = [Strut_O_y1 Strut_O_y1 Strut_O_y2 Strut_O_y2 Strut_O_y1];

%Plot both outer struts.
plot( Strut_O_x_vals,  Strut_O_y_vals) %Plot right OS
plot( -Strut_O_x_vals, Strut_O_y_vals) %Plot left OS

%% Cockpit/Pilot
%To be added at a later date.

%% FRONT VIEW: Plot the centers of gravity! %%
%Center of Wings (NOT CENTER OF GRAVITY)
plot(Target_x,Target_y,'+g')

%Centers of Gravity of Right Wings Spars
Spar_CG_x = [Spar_I_cg_hzc Spar_O_cg_hzc  Spar_I_cg_hzc  Spar_O_cg_hzc];
Spar_CG_y = [Spar_I_cg_vtc Spar_O_cg_vtc -Spar_I_cg_vtc -Spar_O_cg_vtc];
%Centers of Gravity of Right Wings Struts
Strut_CG_x = [Strut_I_cg_hzc  Strut_O_cg_hzc];
Strut_CG_y = [Strut_I_cg_vtc  Strut_O_cg_vtc];
%%%PLOT THESE VALUES%%%
%Right Wing
plot(Spar_CG_x,Spar_CG_y,'+k')
plot(Strut_CG_x,Strut_CG_y,'+k')
%Left Wing
plot(-Spar_CG_x,Spar_CG_y,'+k')
plot(-Strut_CG_x,Strut_CG_y,'+k')

%TailBoom
plot(TailBoom_hzc,TailBoom_vtc,'+k')
```

```
%Horizontal Tail Spar
plot(TailHzSpar_cg_hzc,TailHzSpar_cg_vtc,'+k')

%Vertical Tail Spar
plot(TailVtSpar_cg_hzc,TailVtSpar_cg_vtc,'+k')

%PLOT OVERALL CG OF AIRCRAFT WITHOUT PILOT
CG_ALL_plot = plot(Sum_Hz2,Sum_Vt2,'+r');

%Pilot
%To be added at a later date.

%% FRONT VIEW: Make the graph look nice %%
axis([-400 400 -400 400]) %For unzoomed graph
set( gca, 'FontName', 'Helvetica' );
YLabel = ylabel('Vertical (inches)');
XLabel = xlabel('Spanwise (inches)');
set(XLabel, 'FontName', 'AvantGarde');
set(YLabel, 'FontName', 'AvantGarde');
set(gca, ...
  'TickDir'     , 'out'     , ...
  'TickLength'  , [.02 .02] , ...
  'XMinorTick'  , 'on'      , ...
  'YMinorTick'  , 'on'      , ...
  'LineWidth'   , 1         );

set(CG_ALL_plot, 'LineWidth', 1.5);

set(gcf, 'PaperPositionMode', 'auto');
hold off

%% SIDE VIEW: Draw the 2D Geometry!%%
figure;

%% Tail Boom
%Get the values needed for plotting
TailB_z1 = -TailBoom_InFront;
TailB_z2 = TailB_z1 + TailBoom_Length;
TailB_y1 = TailBoom_vtc-TailBoom_OD/2;
TailB_y2 = TailBoom_vtc+TailBoom_OD/2;
%circle([TailBoom_hzc,TailBoom_vtc],TailBoom_r,100)

%Points to be used in the "box" shape
TailB_z_vals = [TailB_z1 TailB_z2 TailB_z2 TailB_z1 TailB_z1];
TailB_y_vals = [TailB_y1 TailB_y1 TailB_y2 TailB_y2 TailB_y1];

%Plot the Tail Boom
plot(TailB_z_vals,TailB_y_vals)
hold on

%% Plot everything in order to get legend

plot(TailHzSpar_cg_zc,TailHzSpar_cg_vtc,'+k')
plot(Target_z,Target_y,'+g')
```

```
plot(Sum_z,Sum_Vt2,'+r');
legend('Component Geometry', 'Component CG','CG Target', 'Empty Weight CG')

%% Horizontal Tail
% %Get the center location and the circle's radius
% %circle([TailBoom_hzc,TailBoom_vtc],TailBoom_r,100)
% For now, going to make a box, until circle can be fixed....
HzTS_z1 = TailB_z2+TailHz_Location-TailHz_Spar_OD/2;
HzTS_z2 = TailB_z2+TailHz_Location+TailHz_Spar_OD/2; %POSITIVE VALUE

%Points to be used in the "box" shape
HzTailSpar_z_vals = [HzTS_z1 HzTS_z2  HzTS_z2   HzTS_z1  HzTS_z1];
% VtTailSpar_y_vals = [HzTS_y1 HzTS_y1 HzTS_y2  HzTS_y2  HzTS_y1];

plot(HzTailSpar_z_vals,HzTailSpar_y_vals)

%% Vertical Tail
%Get the values needed for plotting
VtTS_z1 = TailB_z2+TailVt_Location-TailVt_Spar_OD/2;
VtTS_z2 = TailB_z2+TailVt_Location+TailVt_Spar_OD/2; %POSITIVE VALUE
% VtTS_y1 = TailVtSpar_cg_vtc + TailVt_Span/2;
% VtTS_y2 = TailVtSpar_cg_vtc - TailVt_Span/2;

%Points to be used in the "box" shape
VtTailSpar_z_vals = [VtTS_z1 VtTS_z2  VtTS_z2   VtTS_z1  VtTS_z1];
% VtTailSpar_y_vals = [VtTS_y1 VtTS_y1 VtTS_y2  VtTS_y2  VtTS_y1];

%Plot the vertical tail
plot(VtTailSpar_z_vals,VtTailSpar_y_vals)

%% Cockpit/Pilot
%To be added at a later date.

%% Wing: Inner Strut(s)
Strut_I_z1 = -Strut_I_OD/2; %Left Val
Strut_I_z2 = Strut_I_OD/2; %Right Val
% Strut_I_y1 = Strut_I_Height/2; %Higher Val
% Strut_I_y2 = -Strut_I_Height/2; %Lower Val

%Points to be used in the "box" shape
Strut_I_z_vals = [Strut_I_z1 Strut_I_z2 Strut_I_z2 Strut_I_z1 Strut_I_z1];
%Strut_I_y_vals = [Strut_I_y1 Strut_I_y1 Strut_I_y2 Strut_I_y2 Strut_I_y1];

%Plot inner strut.
plot( Strut_I_z_vals,  Strut_I_y_vals) %Plot right IS

%% Wing: Inner Spar
%Get the center location and the circle's radius
Spar_I_z = Spar_I_cg_hzc;
Spar_I_y = Spar_I_cg_vtc;
Spar_I_r = Spar_I_OD/2;
%circle([TailBoom_hzc,TailBoom_vtc],TailBoom_r,100)
%FOR NOW, GOING TO MAKE A BOX!
Spar_I_z1 = -Spar_I_OD/2;
Spar_I_z2 = Spar_I_OD/2;
```

```
% Spar_I_y1 = TailBoom_vtc-TailBoom_OD/2;
% Spar_I_y2 = TailBoom_vtc+TailBoom_OD/2;

Spar_I_z_vals = [Spar_I_z1 Spar_I_z2 Spar_I_z2 Spar_I_z1 Spar_I_z1];
% Spar_I_y_vals = [Spar_I_y1 Spar_I_y1 Spar_I_y2 Spar_I_y2 Spar_I_y1];

%Plot both visible spars
plot(Spar_I_z_vals,Spar_I_y_vals)
plot(Spar_I_z_vals,-Spar_I_y_vals)

%% SIDE VIEW: Plot the centers of gravity! %%
%Centers of Gravity of Right Wings Spars
Spar_CG_z = [Spar_I_cg_zc Spar_O_cg_zc  Spar_I_cg_zc  Spar_O_cg_zc];
%         =    72            252           72            252
Spar_CG_y = [Spar_I_cg_vtc Spar_O_cg_vtc -Spar_I_cg_vtc -Spar_O_cg_vtc];
%         =    31.0000       30.8750       -31.0000       -30.8750

%Centers of Gravity of Right Wings Struts
Strut_CG_z = [Strut_I_cg_zc  Strut_O_cg_zc];
%          =    144             360
Strut_CG_y = [Strut_I_cg_vtc  Strut_O_cg_vtc];
%          =    0               0
%%%PLOT THESE VALUES%%%
%Right Wing
plot(Spar_CG_z,Spar_CG_y,'+k')
plot(Strut_CG_z,Strut_CG_y,'+k')

%TailBoom
plot(TailBoom_cg_zc,TailBoom_vtc,'+k')

%Horizontal Tail Spar
plot(TailHzSpar_cg_zc,TailHzSpar_cg_vtc,'+k')

%Vertical Tail Spar
plot(TailVtSpar_cg_zc,TailVtSpar_cg_vtc,'+k')

%PLOT OVERALL CG OF AIRCRAFT
CG_ALL_plot2 = plot(Sum_z,Sum_Vt2,'+r');

%Center of Wing SPARS (NOT CENTER OF GRAVITY)
plot(Target_z,Target_y,'+g')

%% SIDE VIEW: Make the graph look nice %%
axis([-150 250 -200 200]) %For unzoomed graph
set( gca, 'FontName', 'Helvetica' );
YLabel = ylabel('Vertical (inches)');
XLabel = xlabel('"Chordwise" (inches)');
set(XLabel, 'FontName', 'AvantGarde');
set(YLabel, 'FontName', 'AvantGarde');
set(gca, ...
  'TickDir'     , 'out'     , ...
  'TickLength'  , [.02 .02] , ...
  'XMinorTick'  , 'on'      , ...
  'YMinorTick'  , 'on'      , ...
  'LineWidth'   , 1         );
```

```
set(CG_ALL_plot2, 'LineWidth', 1.5);

set(gcf, 'PaperPositionMode', 'auto');
hold off

%% TOP VIEW: Plot the geometry
%Center of wings will be at origin?
figure;

%%Horizontal Tail Spar
%Plot the horizontal tail
HzTailSpar_z_vals2 = [HzTS_z1 HzTS_z1 HzTS_z2 HzTS_z2 HzTS_z1];
plot(HzTailSpar_x_vals,HzTailSpar_z_vals2)
hold on

%% Plot everything in order to get legend

plot(TailHzSpar_cg_hzc,TailHzSpar_cg_zc,'+k')
plot(Target_x,Target_z,'+g')
plot(Sum_Hz2,Sum_z,'+r');
legend('Component Geometry', 'Component CG','CG Target', 'Empty Weight CG')

%% Back to rest of geometry

%%Vertical Tail Spar
%Plot the vertical tail
VtTailSpar_z_vals2 = [VtTS_z1 VtTS_z1 VtTS_z2 VtTS_z2 VtTS_z1];
% TailB_y_vals = [TailB_y1 TailB_y1 TailB_y2 TailB_y2 TailB_y1];
plot(VtTailSpar_x_vals,VtTailSpar_z_vals2)

%%Tail Boom
TailB_z_vals2 = [TailB_z1 TailB_z1 TailB_z2 TailB_z2 TailB_z1];
% TailB_y_vals = [TailB_y1 TailB_y1 TailB_y2 TailB_y2 TailB_y1];
plot(TailB_x_vals,TailB_z_vals2)

%%Wing: Inner Spars
Spar_I_z_vals2 = [Spar_I_z1 Spar_I_z1 Spar_I_z2 Spar_I_z2 Spar_I_z1];
% TailB_y_vals = [TailB_y1 TailB_y1 TailB_y2 TailB_y2 TailB_y1];
plot(Spar_I_x_vals,  Spar_I_z_vals2) %Plot right IS
plot(-Spar_I_x_vals, Spar_I_z_vals2) %Plot left  IS


%%Wing: Inner Struts
%Plot both inner struts.
Strut_I_z_vals2 = [Strut_I_z1 Strut_I_z1 Strut_I_z2 Strut_I_z2 Strut_I_z1];
plot( Strut_I_x_vals,  Strut_I_z_vals2) %Plot right IS
plot( -Strut_I_x_vals, Strut_I_z_vals2) %Plot left IS

%%Wing: Outer Struts
Strut_O_z1 = -Strut_O_OD/2; %Left Val
Strut_O_z2 = Strut_O_OD/2; %Right Val
%Points to be used in the "box" shape
Strut_O_z_vals2 = [Strut_O_z1 Strut_O_z1 Strut_O_z2 Strut_O_z2 Strut_O_z1];
```

```
%Plot outer struts.
plot( Strut_O_x_vals,  Strut_O_z_vals2) %Plot right OS

%%Wing: Outer Spars
Spar_O_z1 = -Spar_O_OD/2;
Spar_O_z2 = Spar_O_OD/2;
Spar_O_z_vals2 = [Spar_O_z1 Spar_O_z1 Spar_O_z2 Spar_O_z2 Spar_O_z1];
%Plot both visible spars
plot(Spar_O_x_vals,Spar_O_z_vals2)
plot(-Spar_O_x_vals,Spar_O_z_vals2)

%% TOP VIEW: Plot the centers of gravity! %%
%%%PLOT THESE VALUES%%%
%Right Wing
plot(Spar_CG_x,Spar_CG_z,'+k')
plot(Strut_CG_x,Strut_CG_z,'+k')

%Left Wing
plot(-Spar_CG_x,Spar_CG_z,'+k')
plot(-Strut_CG_x,Strut_CG_z,'+k')

%TailBoom
plot(TailBoom_hzc,TailBoom_cg_zc,'+k')

%Horizontal Tail Spar
plot(TailHzSpar_cg_hzc,TailHzSpar_cg_zc,'+k')

%Vertical Tail Spar
plot(TailVtSpar_cg_hzc,TailVtSpar_cg_zc,'+k')

%PLOT OVERALL CG OF AIRCRAFT
CG_ALL_plot3 = plot(Sum_Hz2,Sum_z,'+r');

%Center of Wing SPARS (NOT CENTER OF GRAVITY)
plot(Target_x,Target_z,'+g')

%% FRONT VIEW: Make the graph look nice %%
axis([-400 400 -400 400]) %For unzoomed graph

set( gca, 'FontName', 'Helvetica' );
YLabel = ylabel('"Chordwise" (inches)');
XLabel = xlabel('Spanwise (inches)');
set(XLabel, 'FontName', 'AvantGarde');
set(YLabel, 'FontName', 'AvantGarde');
set(gca, ...
  'TickDir'     , 'out'     , ...
  'TickLength'  , [.02 .02] , ...
  'XMinorTick'  , 'on'      , ...
  'YMinorTick'  , 'on'      , ...
  'LineWidth'   , 1         );

set(CG_ALL_plot3, 'LineWidth', 1.5);

set(gcf, 'PaperPositionMode', 'auto');
hold off
```